

000 001 STABILITY, COMPLEXITY AND DATA-DEPENDENT 002 WORST-CASE GENERALIZATION BOUNDS 003 004

005 **Anonymous authors**

006 Paper under double-blind review

007 008 ABSTRACT 009

011 Providing generalization guarantees for stochastic optimization algorithms re-
012 mains a key challenge in learning theory. Recently, numerous works demonstrated
013 the impact of the geometric properties of optimization trajectories on generaliza-
014 tion performance. These works propose worst-case generalization bounds in terms
015 of various notions of intrinsic dimension and/or topological complexity, which
016 were found to empirically correlate with the generalization error. However, most
017 of these approaches involve intractable mutual information terms, which limit a
018 full understanding of the bounds. In contrast, some authors built on algorithmic
019 stability to obtain worst-case bounds involving geometric quantities of a com-
020 binatorial nature, which are impractical to compute. In this paper, we address
021 these limitations by combining empirically relevant complexity measures with a
022 framework that avoids intractable quantities. To this end, we introduce the con-
023 cept of *random set stability*, tailored for the data-dependent random sets produced
024 by stochastic optimization algorithms. Within this framework, we show that the
025 worst-case generalization error can be bounded in terms of (i) the random set
026 stability parameter and (ii) empirically relevant, data- and algorithm-dependent
027 complexity measures of the random set. Moreover, our framework improves exist-
028 ing topological generalization bounds by recovering previous complexity notions
029 without relying on mutual information terms. Through a series of experiments in
030 practically relevant settings, we validate our theory by evaluating the tightness of
031 our bounds and the interplay between topological complexity and stability.

032 1 INTRODUCTION

033
034 Explaining the generalization capabilities of modern deep learning models is still an open problem
035 and an active research area (Zhang et al., 2017; 2021). Classically, supervised learning tasks can be
036 framed as a population risk minimization problem, defined as:

$$037 \min_{w \in \mathbb{R}^d} \{ \mathcal{R}(w) := \mathbb{E}_{z \sim \mu_z} [\ell(w, z)] \}, \quad (1)$$

038 where $z \in \mathcal{Z}$ denotes the data, following a probability distribution μ_z on the data space \mathcal{Z} , and
039 $\ell : \mathbb{R}^d \times \mathcal{Z} \rightarrow \mathbb{R}$ is the loss function. In practice, we have $\mathcal{Z} = \mathcal{X} \times \mathcal{Y}$, where \mathcal{X} denotes a feature
040 space and \mathcal{Y} is a label space. Since μ_z is unknown, it is in general not possible to directly solve
041 Equation (1); instead, we typically solve the *empirical risk minimization problem*: for a dataset
042 $S := (z_1, \dots, z_n) \sim \mu_z^{\otimes n}$ sampled i.i.d. from μ_z , it corresponds to
043

$$044 \min_{w \in \mathbb{R}^d} \{ \widehat{\mathcal{R}}_S(w) := \frac{1}{n} \sum_{i=1}^n \ell(w, z_i) \}. \quad (2)$$

045 To evaluate the validity of this replacement, it is essential to quantify the discrepancy between the
046 two objectives. Thus, a central quantity of interest in learning theory is the *generalization error*,
047 defined as $G_S(w) := \mathcal{R}(w) - \widehat{\mathcal{R}}_S(w)$.

048 To quantify the generalization error, a large body of work analyzes the problem at the level of a single
049 weight vector w by modeling the learning algorithm as a mapping $(S, U) \mapsto w_{S,U}$, where $S \in \mathcal{Z}^n$
050 represents the dataset and U captures the algorithmic randomness. This viewpoint underlies, for
051 example, information-theoretic approaches (Xu & Raginsky, 2017; Steinke & Zakynthinou, 2020;
052 Pensia et al., 2018), as well as the algorithmic stability frameworks (Bousquet & Elisseeff, 2002;
053 Hardt et al., 2016; Feldman & Vondrak, 2019). While these approaches provide generalization

guarantees in various settings, the choice of which iterate to analyze remains unclear in the absence of a stopping criterion, and consequently cannot capture the full behavior of the generalization error.

In contrast to focusing on a single weight vector, recent work has highlighted the role of the *parameter trajectory* – the sequence of iterates generated by the learning algorithm for solving Equation (2) – in explaining the generalization behavior of modern machine learning models (Xu et al., 2024; Fu et al., 2024; Andreeva et al., 2024). Indeed, since the empirical risk can contain many local minima, the trajectory surrounding a local minimum offers a concise way to assess its quality. The trajectory itself inherently reflects the influence of the optimization algorithm, the choice of hyperparameters, and the dataset, factors that are essential for deriving meaningful generalization bounds.

To capture the geometric information of the *parameter trajectory*, several authors have proposed analyzing the *worst-case* generalization error along the entire trajectory, rather than relying on a single weight vector. Due the dependence of the parameter trajectory on the random variables S (dataset) and U (algorithmic noise), numerous studies on worst-case generalization bounds adopted the formulation of *data-dependent random sets* (Simsekli et al., 2020; Dupuis et al., 2023; Andreeva et al., 2023). In line with these previous works, we formalize a learning algorithm as a mapping,

$$\mathcal{A} : \bigcup_{n \geq 1} \mathcal{Z}^n \times \Omega \longrightarrow \text{CL}(\mathbb{R}^d) := \{\text{closed subsets in } \mathbb{R}^d\}, \quad \mathcal{A} : (S, U) \longmapsto \mathcal{W}_{S,U}, \quad (3)$$

where $S \in \mathcal{Z}^n$ is the dataset and $U \in \Omega$ is an independent random variable representing the algorithm randomness. This formalization includes (but is not limited to) the following examples.

Example 1.1. Consider a stochastic optimizer $w_{k+1} = F(w_k, S, U)$ (U is the batch noise) and $K_1, K_2 \in \mathbb{N}^*$. The parameter trajectory is defined as $\mathcal{A}(S, U) = \mathcal{W}_{S,U} := \{w_k, K_1 \leq k \leq K_2\}$.

Example 1.2. Consider a dynamics of the form $dW_t = -\nabla \mathcal{R}_S(W_t)dt + \sigma dB_t$, where $U := (B_t)_{t \geq 0}$ is a Brownian motion. Let $T > 0$, the parameter trajectory is $\mathcal{W}_{S,U} := \{W_t, t \in [0, T]\}$.

The following Examples 1.3 and 1.4 illustrate that this formulation also includes classical learning-theoretic frameworks.

Example 1.3. Singleton bounds correspond to the case where we choose $\mathcal{A}(S, U) := \{w_{S,U}\}$.

Example 1.4. Classical worst-case (uniform) generalization error over a data-independent hypothesis set \mathcal{W} (Shalev-Shwartz & Ben-David, 2014) correspond to a constant mapping $\mathcal{A}(S, U) = \mathcal{W}$.

In this general setting, the main quantity of interest is the *worst-case generalization error* over $\mathcal{W}_{S,U}$,

$$G_S(\mathcal{W}_{S,U}) := \sup_{w \in \mathcal{W}_{S,U}} (\mathcal{R}(w) - \widehat{\mathcal{R}}_S(w)). \quad (4)$$

In the case of Example 1.4, this problem has been classically analyzed through the Rademacher complexity over \mathcal{W} (Bartlett & Mendelson, 2002). However, as noted by Dupuis et al. (2023), these classical techniques break down for data-dependent random sets.

To overcome this limitation, many studies have employed information-theoretic techniques, particularly within the “fractal-based” literature (Simsekli et al., 2020; Birdal et al., 2021). A unifying perspective recently emerged with the PAC-Bayesian theory for random sets (Dupuis et al., 2024), which was recently employed by Andreeva et al. (2024) to establish generalization bounds based on novel topological complexity measures. Informally, all these bounds are of the following form¹:

$$\sup_{w \in \mathcal{W}_{S,U}} (\mathcal{R}(w) - \widehat{\mathcal{R}}_S(w)) \lesssim \sqrt{\frac{\mathbf{C}(\mathcal{W}_{S,U}) + \text{IT} + \log(1/\zeta)}{n}}, \quad (5)$$

with probability at least $1 - \zeta$. The term *IT* is an *information-theoretic* (IT) term, typically the *total* mutual information between the dataset S and the set $\mathcal{W}_{S,U}$. The aforementioned bounds differ in the choice of complexity measure $\mathbf{C}(\mathcal{W}_{S,U})$, but all include an IT term. For concrete examples, we refer the reader to (Dupuis et al., 2023; 2024; Andreeva et al., 2024). The presence of such IT term is a major drawback of these studies, as it is computationally intractable and not well-understood in the general case (Dupuis et al., 2024), and they can potentially be infinite.

On the other hand, Foster et al. (2019) adopted a conceptually different approach by extending the notion of algorithmic stability (Bousquet & Elisseeff, 2002) to data-dependent hypothesis sets. Despite allowing a different point of view on Equation (4), their assumption does not explicitly take into

¹We use the notation \lesssim in informal statements where absolute constants have been omitted.

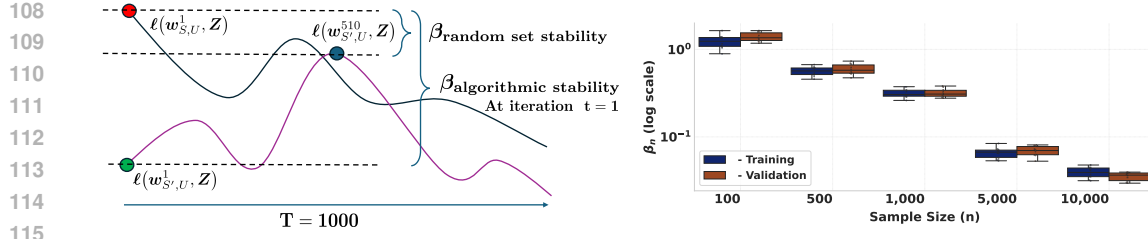


Figure 1: (Left) Evolution of the loss function $\ell(\cdot, Z)$ for a fixed sample $Z \in \mathcal{Z}$ over $T = 1000$ iterations, for two neighboring datasets $S, S' \in \mathcal{Z}^n$. While the classical notion of algorithmic stability measures the error at a specific iteration t , our stability notion extends this perspective to the entire training trajectory. (Right) Numerical estimation of our new random set stability parameter (β_n) as n increases. The experiments demonstrate that β_n decreases with larger n .

account the algorithm randomness U , which is known to be paramount for deriving stability-based bounds (Hardt et al., 2016). Moreover, Foster et al. (2019) use a modified notion of Rademacher complexity whose evaluation requires all sets² of the form \mathcal{W}_{S^σ} , where $S_\sigma = (z_{1,\sigma_1}, \dots, z_{n,\sigma_n})$, with $S_1 := (z_{1,1}, \dots, z_{n,1}), S_{(-1)} := (z_{1,-1}, \dots, z_{n,-1}) \sim \mu_z^{\otimes n}$ and $\sigma \in \{-1, 1\}^n$. Hence, the sets \mathcal{W}_{S^σ} differ from the empirically accessible set $\mathcal{W}_{S,U}$ and evaluating all sets \mathcal{W}_{S^σ} would require running the training algorithm exponentially many times in n , rendering this approach impractical. A similar construction has been used by Sachs et al. (2023) in the definition of the algorithmic-dependent Rademacher complexity.

Contributions. In this study, we propose to address the aforementioned issues by introducing a novel framework for deriving worst-case generalization bounds on data-dependent random sets, which are empirically relevant and do not contain intractable mutual information terms. Inspired by Foster et al. (2019), we adopt a stability-based approach, which we adapt to exploit the algorithm randomness in an explicit way. Based on our new assumption, we show that $G_S(\mathcal{W}_{S,U})$ can be upper bounded in terms of the stability parameter and a Rademacher complexity term. This allows us to take advantage of the best of both worlds by (1) avoiding the intricate information-theoretic (IT) terms and (2) relating the generalization error to topologically meaningful complexity measures, hence, providing IT-terms free versions of the topological generalization bounds of Birdal et al. (2021); Andreeva et al. (2024). Our contributions are detailed below.

- We introduce the notion of *random set stability*, specifically designed for stochastic learning algorithms. More precisely, we define a new stability parameter β_n measuring how much the random set $\mathcal{W}_{S,U}$ changes if we replace one or more data points in S , in a sense that is formally introduced in Assumption 3.1 below. Moreover, we relate β_n to classical stability notions, providing a systematic procedure to establish random set stability in diverse settings.
- We derive an expected worst-case generalization bound in terms of a Rademacher complexity term evaluated over the empirically relevant set $\mathcal{W}_{S,U}$ and the stability parameter.
- We apply our framework to obtain generalization bounds based on the fractal and topological complexity measures introduced in (Birdal et al., 2021; Andreeva et al., 2024) without any intractable mutual information terms. These bounds read as follows:

$$\mathbb{E} \left[\sup_{w \in \mathcal{W}_{S,U}} (\mathcal{R}(w) - \widehat{\mathcal{R}}_S(w)) \right] \lesssim \beta_n^{1/3} \left(1 + \mathbb{E} \left[\sqrt{\log \mathbf{C}(\mathcal{W}_{S,U})} \right] \right),$$

where β_n is the stability parameter and $\mathbf{C}(\mathcal{W}_{S,U})$ is the complexity measure (see Section 4). Therefore, we provide the first fully computable topological bounds for practically used optimization algorithms, hence, addressing the main issues of the aforementioned previous works.

- We provide a systematic empirical investigation of the tightness of our bounds.
- We empirically investigate the previously introduced topological quantities and their interplay with stability as the sample size n varies, extending the correlation analyses of prior studies, and therefore providing evidence supporting the validity of our stability-based approach.

The implementation will be made available upon publication. All proofs are in the appendix.

² \mathcal{W}_S denotes in the setting of (Foster et al., 2019) a data dependent hypothesis set. The authors do not account for algorithmic randomness U . For U constant both notation can be seen as equivalent.

162 **2 TECHNICAL BACKGROUND**

164 In this section, we provide some technical background on algorithmic stability. One of our contributions,
 165 described in Section 3.1, is to extend these notions to data-dependent random sets.

166 Algorithmic stability is a fundamental concept in learning theory (Bousquet & Elisseeff, 2002; Bous-
 167 quet et al., 2020). It has proven successful in providing generalization guarantees for widely used
 168 stochastic optimization algorithms Feldman & Vondrak (2019); Zhu et al. (2023); Hardt et al. (2016).
 169 To position our work within existing stability-based bounds, we consider a variant of *algorithmic*
 170 *stability*, called *uniform argument stability* Bassily et al. (2020). As with most stability notions,
 171 it is defined with respect to a single iteration. Therefore, the learning algorithm used in the next
 172 definition corresponds to the setting of Example 1.3 and can be seen as a randomized mapping
 173 $(S, U) \mapsto \mathcal{A}(S, U) \in \mathbb{R}^d$. In all the following, we say that two datasets $S, S' \in \mathcal{Z}^n$ are neighbor-
 174 ing datasets if they differ by one element, which we denote $S \simeq S'$.

175 **Definition 2.1.** Let $\mathcal{A} : (S, U) \rightarrow \mathbb{R}^d$ be a randomized algorithm. \mathcal{A} satisfies β -uniform argument
 176 stability if for any neighboring datasets $S \simeq S'$, we have $\mathbb{E}_U [\|\mathcal{A}(S, U) - \mathcal{A}(S', U)\|] \leq \beta$.

177 If $\ell(w, z)$ is L -Lipschitz continuous in w , this implies the algorithmic stability Hardt et al. (2016):

$$\sup_{S \simeq S'} \sup_{z \in \mathcal{Z}} \mathbb{E}_U [\ell(\mathcal{A}(S, U), z) - \ell(\mathcal{A}(S', U), z)] \leq L\beta. \quad (6)$$

181 In the context of worst-case generalization bounds, where $\mathcal{W}_{S, U}$ is a set (i.e., not a singleton), one
 182 needs to specify the stability of the entire set $\mathcal{W}_{S, U}$. To address this issue, a first step was taken by
 183 Foster et al. (2019), who introduced the following notion of hypothesis set stability.

184 **Definition 2.2.** A family $(\mathcal{W}_S)_{S \in \mathcal{Z}^n} \in (\mathbb{R}^d)^{\mathcal{Z}^n}$ of data-dependent hypothesis sets is β -uniformly
 185 stable when for any $S \simeq S'$ in \mathcal{Z}^n and $w \in \mathcal{W}_S$, there exists $w' \in \mathcal{W}_{S'}$ such that:

$$\sup_{z \in \mathcal{Z}} |\ell(w, z) - \ell(w', z)| \leq \beta.$$

188 Although this assumption has been analyzed in settings such as strongly convex optimization (Foster
 189 et al., 2019), the notion of *hypothesis set stability* (Definition 2.2) does not account for the presence
 190 of algorithmic randomness U and therefore cannot be applied to the data-dependent random sets
 191 defined by Equation (3). In Section 3, we thus extend Definition 2.2 to data-dependent random sets.

192 **3 MAIN THEORETICAL RESULTS**

194 In this section, we present our main theoretical contributions, which consist in deriving expected
 195 worst-case generalization bounds through a new concept of random set stability, described in Sec-
 196 tion 3.1. After discussing its validity, we present a key technical lemma and recover classical gener-
 197 alization bounds in the case of Examples 1.3 and 1.4. We then apply our framework to improve sev-
 198 eral data-dependent worst-case generalization bounds, including intrinsic dimension bounds Sim-
 199 sekli et al. (2020); Birdal et al. (2021) and topological bounds Andreeva et al. (2024).

201 **3.1 RANDOM SET STABILITY**

203 As explained above, the main drawback of Definition 2.2 is that it does not explicitly account for the
 204 algorithm randomness (e.g., batch indices), while algorithmic randomness is known to be paramount
 205 for single-iterates stability bounds Hardt et al. (2016); Zhu et al. (2023).

206 To address this issue, we propose an improvement of the assumption of Foster et al. (2019), account-
 207 ing for the presence of randomness. The main difficulty that arises here is to give a meaning to the
 208 expressions such as “for all $w \in \mathcal{W}_{S, U}$ ”, when $\mathcal{W}_{S, U}$ is a random set. To do so, we define the notion
 209 of data-dependent selection Molchanov (2017).

210 **Definition 3.1.** A data-dependent selection of $\mathcal{W}_{S, U}$ is a deterministic mapping $\omega : \text{CL}(\mathbb{R}^d) \times \mathcal{Z}^n \rightarrow$
 211 \mathbb{R}^d such that $\omega(\mathcal{W}_{S, U}, S') \in \mathcal{W}_{S, U}$, almost surely. In particular, we assume the existence of a
 212 random variable $\omega_0(\mathcal{W}_{S, U}, S')$ such that, almost surely, $\omega_0(\mathcal{W}_{S, U}, S') \in \arg \max_{w \in \mathcal{W}_{S, U}} G_{S'}(w)$,
 213 where we recall that $G_{S'}(w) := \mathcal{R}(w) - \hat{\mathcal{R}}_{S'}(w)$ for all $S' \in \mathcal{Z}^n$.

214 Note that the existence of such a random variable is ensured under mild measure-theoretic conditions
 215 Molchanov (2017). Equipped with this definition, we now introduce our stability assumption.

216 **Assumption 3.1** (Random set stability). *Algorithm \mathcal{A} is β_n -random set stable if for any $J \in \mathbb{N}^*$ and*
 217 *any data-dependent selection ω of $\mathcal{W}_{S,U}$, there exists a map $\omega' : \text{CL}(\mathbb{R}^d) \times \mathbb{R}^d \rightarrow \mathbb{R}^d$ such that:*

218 • For any S, U and $w \in \mathbb{R}^d$, $\omega'(\mathcal{W}_{S,U}, w) \in \mathcal{W}_{S,U}$.
 219 • For all $z \in \mathcal{Z}$ and two datasets $S, S' \in \mathcal{Z}^n$ differing by J elements we have:

220
$$\mathbb{E}_U[|\ell(\omega(\mathcal{W}_{S,U}, S), z) - \ell(\omega'(\mathcal{W}_{S',U}, \omega(\mathcal{W}_{S,U}, S)), z)|] \leq \beta_n J.$$

223 In the absence of algorithmic randomness (i.e., when U is constant), Assumption 3.1 is a particular
 224 case of Definition 2.2. Stability assumptions are usually enounced for neighboring datasets; here,
 225 we present a variant with datasets differing by J elements. These two variants are equivalent, and we
 226 choose this presentation to simplify subsequent proofs and notations. The presence of the mapping
 227 ω' might be intriguing: ω' corresponds to the parameter denoted w' in Definition 2.2 and is denoted
 228 this way to make its dependence on the different random variables explicit.

229 **Applicability of random set stability.** The question naturally arises as to whether this assumption
 230 can be met and how it fits within the existing stability conditions. We answer this question with the
 231 following lemma, which shows that Assumption 3.1 is implied by Definition 2.1.

232 **Lemma 3.2.** *Consider a fixed $K \in \mathbb{N}^*$, $1 \leq k \leq K$, and algorithms³ $\mathcal{A}_k(S, U) := w_k$. Let*
 233 *$\mathcal{A}(S, U) = \mathcal{W}_{S,U} = \{\mathcal{A}_k(S, U)\}_{k=1}^K$ be an algorithm in the sense of Equation (3). Assume that for*
 234 *all k , \mathcal{A}_k is δ_k -uniformly argument-stable in the sense of Definition 2.1 and that the loss $\ell(w, z)$ is L -*
 235 *Lipschitz-continuous in w . Then, \mathcal{A} is random set stable with parameter at most $\beta_n = L \sum_{k=1}^K \delta_k$.*

236 In the context of Example 1.1, this result shows that Definition 2.1 implies random set stability. It
 237 can be noted that many stability-based studies rely on a Lipschitz assumption and prove uniform
 238 argument stability to derive algorithmic stability parameters Hardt et al. (2016), as noted by Bassily
 239 et al. (2020). Therefore, we see that the conditions of Lemma 3.2 can be satisfied in numerous cases,
 240 such as optimization of convex, smooth, and Lipschitz continuous functions Hardt et al. (2016).
 241 Under these conditions, it is obtained that the stability parameter is of order $\delta_k = \mathcal{O}(k/n)$, hence,
 242 yielding random set stability with a parameter of order $\mathcal{O}(T^2/n)$, in the worst case.

243 **Projected SGD.** Fix $T \in \mathbb{N}$. Let us consider the projected SGD recursion on a loss function ℓ , which
 244 can be non-convex, i.e., given a dataset $S = (z_1, \dots, z_n) \in \mathcal{Z}^n$, consider the following algorithm:

245 $w_{k+1} = \Pi_R [w_k - \eta_k \nabla \ell(w_k, z_{i_{k+1}})]$, $\mathcal{A}_{\text{SGD}}(S, U) = \mathcal{W}_{S,U} := \{w_1, \dots, w_T\}$ (7)

246 where $i_k \sim \mathcal{U}(\{1, \dots, n\})$ are random indices, $U := \{i_k\}_{k \geq 1}$, and Π_R is the projection on the ball
 247 $\bar{B}_R(0)$. The next corollary uses Lemma 3.2 to establish the random set stability of SGD for Lipschitz
 248 and smooth losses, and is an adaptation of (Hardt et al., 2016, Theorem 3.12) to our setting.

249 **Corollary 3.3.** *Suppose that, for all z , $\ell(\cdot, z)$ is L -Lipschitz, $\nabla \ell(\cdot, z)$ is G -Lipschitz, and that $\eta_k \leq$
 250 c/k for some $c < 1/G$. Then, \mathcal{A}_{SGD} is random-set-stable with parameter*

251
$$\beta_n = \frac{4LR}{n-1} \left(\frac{L}{GR} \right)^{1/Gc+1} \sum_{1 \leq k \leq T} k^{\frac{Gc}{Gc+1}}.$$

252 3.2 WORST-CASE GENERALIZATION BOUND FOR DATA-DEPENDENT STABLE RANDOM SETS

253 We now leverage Assumption 3.1 to prove worst-case generalization bounds over random sets. The
 254 next lemma shows that the expected worst-case generalization error can be bounded in terms of the
 255 random set stability parameter and a Rademacher complexity term (Bartlett & Mendelson, 2002).

256 **Lemma 3.4.** *Let $S \sim \mu_z^{\otimes n}$. Let $J, K \in \mathbb{N}^*$ be such that $n = JK$, and $\tilde{S}_J \sim \mu_z^{\otimes J}$ be independent of
 257 S and U . Assume that algorithm \mathcal{A} satisfies Assumption 3.1 with parameter $\beta_n > 0$, then:*

258
$$\mathbb{E} [\sup_{w \in \mathcal{W}_{S,U}} (\mathcal{R}(w) - \hat{\mathcal{R}}_S(w))] \leq 2\mathbb{E} [\text{Rad}_{\tilde{S}_J}(\mathcal{W}_{S,U})] + 2J\beta_n,$$
 (8)

259 where $\text{Rad}_S(\mathcal{W})$ denotes the Rademacher complexity, whose definition is recalled in Definition A.1.

260 Most existing data-dependent worst-case generalization bounds rely on an information-theoretic
 261 approach Simsekli et al. (2020); Hodgkinson et al. (2022); Andreeva et al. (2024). In particular, this
 262 theorem can be seen as an analog of (Dupuis et al., 2024, Theorem 6), which provided a bound in

263 ³ \mathcal{A}_k is an algorithm with values in \mathbb{R}^d , i.e., its output is the k -th iterate of the optimization algorithm.

270 terms of Rademacher complexity and information-theoretic terms. Instead of information-theoretic
 271 terms, our framework makes use of the random set stability parameter β_n .
 272

273 In Lemma 3.4, the number J is a free parameter. Before discussing the main applications of our
 274 methods, we show that a certain choice of J recovers: (1) classical algorithmic stability bounds
 275 ($J = 1$) and (2) worst-case bounds over fixed hypothesis sets ($J = n$). Therefore, the parameter J
 276 can be seen as interpolating between these two settings, while yielding new data-dependent worst-
 277 case generalization bounds for intermediary values of J .
 278

278 **Corollary 3.5** (Recovering stability bounds). *Consider an algorithm \mathcal{A} as in Example 1.3 and as-
 279 sume that \mathcal{A} satisfies Assumption 3.1 with parameter β_n . Then, \mathcal{A} is algorithmically stable in the
 280 sense of Equation (6). By setting $J = 1$ in Lemma 3.4, we obtain:*

$$281 \mathbb{E}[\mathcal{R}(\mathcal{A}(S, U)) - \widehat{\mathcal{R}}_S(\mathcal{A}(S, U))] \leq 2\beta_n. \\ 282$$

283 Up to the absolute constant 2, this recovers classical algorithmic stability-based expected general-
 284 ization bounds Bousquet & Elisseeff (2002); Bassily et al. (2020).
 285

286 **Corollary 3.6** (Recovering bounds on fixed hypothesis sets). *Consider the setting of Example 1.4.
 287 Then, the algorithm satisfies Assumption 3.1 with parameter $\beta_n = 0$. By using $J = n$ we obtain:*

$$288 \mathbb{E}[\sup_{w \in \mathcal{W}} (\mathcal{R}(w) - \widehat{\mathcal{R}}_S(w))] \leq 2\mathbb{E}[\text{Rad}_S(\mathcal{W})], \\ 289$$

290 where we observe that $\tilde{S}_n \sim \mu_z^{\otimes n}$ and $S \sim \mu_z^{\otimes n}$ have the same distribution.
 291

292 We observe that when $\beta_n = \mathcal{O}(n^{-1})$, Corollary 3.5 recovers the classical convergence rate of Hardt
 293 et al. (2016). Corollary 3.6 shows that our framework tightly recovers the classical Rademacher
 294 complexity bounds (for fixed hypothesis set \mathcal{W}) Bartlett & Mendelson (2002), as well as all known
 295 consequences of these bounds, such as VC dimension bounds (Vapnik & Vapnik, 1998) and covering
 296 number bounds (Shalev-Shwartz & Ben-David, 2014). In particular, Corollary 3.6 shows that in the
 297 data-independent case we obtain the usual worst-case convergence rate of $\mathcal{O}(n^{-1/2})$.
 298

299 4 APPLICATIONS

300 In this section, we apply our random set stability framework to improve recently proposed data-
 301 dependent worst-case generalization bounds in terms of fractal dimensions and topological com-
 302 plexities Andreeva et al. (2024). We assume that a learning algorithm $\mathcal{A}(S, U) =: \mathcal{W}_{S,U}$ is given,
 303 in the sense of Equation (3). One may think of $\mathcal{W}_{S,U}$ as a learning trajectory as in Example 1.1.
 304

305 **Assumptions.** Before presenting our main applications, we introduce some structural assumptions.
 306 We first note that the Rademacher complexity (RC) term appearing in Lemma 3.4 is computed using
 307 a sample $\tilde{S}_J \sim \mu_z^{\otimes J}$ independent of the random set $\mathcal{W}_{S,U}$. Despite this, the set over which the RC
 308 term is computed is the data-dependent random set $\mathcal{W}_{S,U}$, while the independent sample \tilde{S}_J is only
 309 used to evaluate the loss inside the RC. In order to exploit this property, we assume that the loss has
 310 a ‘‘local’’ Lipschitz regularity, in the following sense.
 311

312 **Assumption 4.1** (Lipschitz on random sets). *There exists a measurable map $(S, U) \mapsto L_{S,U}$ such
 313 that for all S and all U , for all $w, w' \in \mathcal{W}_{S,U}$, for all $z \in \mathcal{Z}$, $|\ell(w, z) - \ell(w', z)| \leq L_{S,U} \|w - w'\|$.*
 314

315 Lipschitz continuity assumptions are commonly used in the context data-dependent worst-case
 316 bounds Simsekli et al. (2020); Birdal et al. (2021); Andreeva et al. (2023). However, our framework
 317 crucially only requires the Lipschitz continuity of $\ell(\cdot, z)$ to hold on each set $\mathcal{W}_{S,U}$ individually, with
 318 a Lipschitz constant $L_{S,U}$ that depends both on the dataset $S \in \mathcal{Z}^n$ and the noise U . Note however
 319 that this local Lipschitz continuity of $\ell(\cdot, z)$ is still required to be uniform in $z \in \mathcal{Z}$. For instance,
 320 in the case of Example 1.1, where $\mathcal{W}_{S,U}$ is finite, then Assumption 4.1 is satisfied as soon as \mathcal{Z} is
 321 finite (or compact if $z \mapsto \nabla \ell(w, z)$ is continuous for a topology on \mathcal{Z}).
 322

323 As is typical in this literature Andreeva et al. (2024); Dupuis et al. (2024); Birdal et al. (2021);
 324 Bartlett & Mendelson (2002), we also assume the boundedness of the loss function.
 325

326 **Assumption 4.2.** *We assume that the loss ℓ is bounded in $[0, B]$, with $B > 0$ being a constant.*
 327

324
325

4.1 INTRINSIC DIMENSIONS AND TOPOLOGICAL BOUNDS

326 Recent studies Simsekli et al. (2020); Dupuis et al. (2023); Andreeva et al. (2023); Dupuis et al.
 327 (2024); Birdal et al. (2021); Andreeva et al. (2024) have established upper-bounds on Equation (4)
 328 and drawn links between the *topological structure* of $\mathcal{W}_{S,U}$ and the generalization error. These
 329 bounds are of the form presented in Equation (5). As mentioned in Section 1, one of the main
 330 drawbacks of these bounds is that they contain intractable and poorly understood mutual information
 331 terms. One of our main contributions is to show that, under random set stability, we are able to obtain
 332 data-dependent worst-case generalization bounds featuring many of the most popular complexity
 333 measures, without the need of the intractable mutual information terms (denoted IT in Equation (5)).

334 We first present an adaptation to our setting of the intrinsic dimension-based bounds of (Simsekli
 335 et al., 2020), without any mutual information term.

336 **Theorem 4.3.** *Suppose that Assumptions 4.2, 3.1, and 4.1 hold, and that $\mathcal{W}_{S,U}$ is a.s. of finite
 337 diameter. Without loss of generality, assume that $\beta_n^{-2/3}$ is an integer divisor of n . There exists
 338 $\delta_n > 0$ such that for all $\delta < \delta_n$*

$$339 \mathbb{E} \left[\sup_{w \in \mathcal{W}_{S,U}} (\mathcal{R}(w) - \widehat{\mathcal{R}}_S(w)) \right] \leq 2\mathbb{E} \left[\frac{B}{n} + \delta L_{S,U} + \beta_n^{1/3} \left(1 + B \sqrt{4\overline{\dim}_B(\mathcal{W}_{S,U}) \log \frac{1}{\delta}} \right) \right],$$

340 where $\overline{\dim}_B(\mathcal{W}_{S,U})$ is the upper box-counting dimension (Falconer, 2013), which we define in the
 341 appendix in Definition A.4. We refer to the Appendix B.4 for a discussion of the parameter δ_n .

342 In many cases, the upper box-counting dimension of $\mathcal{W}_{S,U}$ is much smaller than the ambient dimension d (Falconer, 2013). Under mild assumptions, the upper box-counting dimension can be
 343 replaced by other notions like the persistent homology dimension (Birdal et al., 2021) and the magnitude dimension (Andreeva et al., 2023), which have provided promising empirical results.

344 However, it was argued by Andreeva et al. (2024) that such intrinsic dimensions are not well-suited
 345 to the practically used stochastic optimizers due to their discrete nature, as for instance in Exam-
 346 ple 1.1. To overcome this issue, these authors proposed to use two new notions of topological
 347 complexity, called the α -weighted lifetime sums (denoted $\mathbf{E}^\alpha(\mathcal{W}_{S,U})$) and the positive magnitude
 348 (denoted $\mathbf{PMag}(s \cdot \mathcal{W}_{S,U})$), and significantly improved the empirical results. Intuitively, the α -
 349 weighted lifetime can be understood as tracking the evolution of ‘connected components’ of a set
 350 across different scales and summing their contributions. On the other hand, the magnitude may be
 351 thought of as capturing the effective number of distinct points in a finite space at different scale
 352 Leinster (2013). We defer a precise definition of these notions to Definition A.6 and A.9.

353 In the next theorem, we provide IT free versions of the topological generalization bounds of An-
 354 dreeva et al. (2024) under our assumption of random set stability (Assumption 3.1).

355 **Theorem 4.4.** *Suppose that Assumptions 4.2, 3.1, and 4.1 hold. We further assume that the set
 356 $\mathcal{W}_{S,U}$ is almost surely finite. Without loss of generality, assume that $\beta_n^{-2/3}$ is an integer divisor of
 357 n . Then, for any $\alpha \in (0, 1]$, we have*

$$358 \mathbb{E} \left[\sup_{w \in \mathcal{W}_{S,U}} (\mathcal{R}(w) - \widehat{\mathcal{R}}_S(w)) \right] \leq \beta_n^{1/3} \left(2 + 2B + 2B\mathbb{E} \left[\sqrt{2 \log(1 + K_{n,\alpha} \mathbf{E}^\alpha(\mathcal{W}_{S,U}))} \right] \right),$$

359 where $K_{n,\alpha} := 2(2L_{S,U}\sqrt{n}/B)^\alpha$. Moreover, for any $\lambda > 0$, let $s(\lambda) := \lambda L_{S,U}\beta_n^{-1/3}/B$. We have

$$360 \mathbb{E} \left[\sup_{w \in \mathcal{W}_{S,U}} (\mathcal{R}(w) - \widehat{\mathcal{R}}_S(w)) \right] \leq \beta_n^{1/3} \left(2 + \lambda B + \frac{2B}{\lambda} \mathbb{E} [\log \mathbf{PMag}(s(\lambda) \cdot \mathcal{W}_{S,U})] \right).$$

361 This result suggests that a theoretically justified choice of the magnitude scale would be $s(\lambda) \approx$
 362 $\beta_n^{-1/3}$, which amounts to $\Theta(n^{1/3})$ in the event that $\beta_n = \mathcal{O}(1/n)$. As a reminder, in the classical
 363 setting Corollary 3.6 we recover the standard convergence rate of $\mathcal{O}(n^{-1/2})$.

364 Unlike trajectory-dependent topological bounds Simsekli et al. (2020); Birdal et al. (2021); Dupuis
 365 et al. (2023); Andreeva et al. (2024), our bounds do not involve IT terms, which can be unbounded.
 366 While our bounds result in a slower convergence rate, this represents a deliberate trade-off to main-
 367 tain boundedness. In addition to replacing IT terms with a stability assumption, the stability param-
 368 eter β_n acts as a multiplying constant in the bound, hence increasing the impact of the topological

378 complexity on the bound. Compared to the IT terms, β_n is easily interpretable and can be expected
 379 to decrease with n at a polynomial rate, as discussed above.
 380

381 5 EMPIRICAL EVALUATIONS

383 In Section 4, we provided the first fully computable topological/worst-case generalization bounds,
 384 without the need for intractable mutual information terms, which limited the empirical analysis of
 385 previous works. Instead, our bounds are mainly based on the stability parameter β_n , which allows us
 386 to assess how they empirically compare with the worst-case generalization error and whether their
 387 structure aligns with observations, thus validating the framework and its practical applicability.
 388

389 All experiments are performed using a Vision Transformer (ViT) Dosovitskiy et al. (2021) on the
 390 CIFAR-100 dataset and GraphSAGE Hamilton et al. (2017) on the MNISTSuperpixels dataset Monti
 391 et al. (2017). All models are implemented in PyTorch and trained with the ADAM optimizer
 392 (Kingma & Ba, 2014). Further implementation details for both models are provided in Appendix C.
 393

394 **Experimental Design.** We follow the protocol of previous works Dupuis et al. (2023); Andreeva
 395 et al. (2024) and train models until convergence, using this checkpoint as a starting point for further
 396 analysis. Our empirical analysis is structured in two main parts.
 397

398 First, we analyze the order of magnitude of our bounds, offering initial insights into the tightness
 399 of our framework. We fine-tune each model for 500 iterations on a previously unseen dataset, with
 400 fixed batch sizes (b) and learning rates (η), in particular $b \in \{64, 128\}$ and $\eta \in \{10^{-6}, 10^{-5}\}$. For
 401 each (b, η) configuration, we estimate the stability coefficient Assumption 3.1 over 5 different seeds.
 402

403 Then we examine the relationship between stability and topological complexity (i.e., weighted life-
 404 time sums and positive magnitude in Theorem 4.4). This analysis is motivated by the dependence
 405 of the stability parameter on the sample size n and the multiplicative interaction between stability
 406 and topological complexity in Theorem 4.4. To this end, we fine-tune the models for further $5 \cdot 10^3$
 407 iterations. The experiments are structured on a $4 \times 4 \times 5$ grid based on the learning rate η , the batch
 408 size b , and n . For detailed information about the hyperparameter, we refer to Appendix C.
 409

410 **Quantity Estimation.** In this paragraph, we describe the quantities used in our empirical analysis
 411 and their estimation. Implementation details are provided in the Appendix.
 412

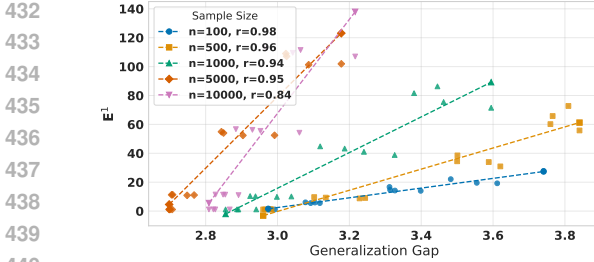
- 413 • **Generalization error:** We approximate $G_S(\mathcal{W}_{S,U})$ (Equation (4)) by tracking train and test risk
 414 at every iteration and reporting $\max_t\{\text{test risk} - \text{train risk}\}$. This refines prior proxies
 415 based on either the final gap Birdal et al. (2021) or the worst test risk Andreeva et al. (2024).
 416 • **Topological complexities:** We compute $\text{PMag}(\mathcal{W}_{S,U})$ via a Krylov subspace PCG approxima-
 417 tion Salim (2021), and $\mathbf{E}^\alpha(\mathcal{W}_{S,U})$ using giotto-ph Pérez et al. (2021) with $\alpha = 1$.
 418 • **Distance matrix:** For trajectories $\mathcal{W}_{S,U}$, we form a Euclidean distance matrix $\rho(w, w') = \|w - w'\|$. To reduce computational cost, we uniformly sample 1500 of the 5000 iterations.
 419 • **Stability parameter:** For random set stability (Assumption 3.1), we replace 50 unseen samples
 420 per training set, retrain to obtain $\mathcal{W}_{S,U}$ and $\mathcal{W}_{S',U}$, and measure worst-case loss deviations across
 421 iterations $\max_{w \in \mathcal{W}_{S,U}} \min_{w' \in \mathcal{W}_{S',U}} \sup_{Z \in \mathcal{Z}} |\ell(w, Z) - \ell(w', Z)|$. With $M = 500$ held-out
 422 points \mathbf{Z} (see Algorithm 1), we average results over 5 different random seeds. **Note that this**
 423 **method necessarily leads to an optimistic estimation of the stability parameter β_n , as it would be**
 424 **intractable to evaluate the supremum over the entire data space \mathcal{Z} .**

425 5.1 RESULTS AND DISCUSSION

426 We now present our main empirical results. First, we numerically evaluate our bounds. Next, we
 427 investigate the interplay between stability and the topological quantities appearing in Theorem 4.4.
 428

429 **Order of the bounds.** Our goal is to have an estimate of the order of magnitude of the worst-
 430 case error predicted by our bounds. To avoid the computationally costly evaluation of Lipschitz
 431 constants, we estimate a simple upper bound on the Rademacher complexity that is common to all
 432 our theoretical results. Concretely, we use Massart’s lemma (Shalev-Shwartz & Ben-David, 2014)
 433 to bound the right-hand side of Equation (8) by $2\sqrt{2\log(T)/J} + 2J\beta_n$, where T is the number of
 434 iterations. We estimate β_n using the procedure above and optimize over J (see Appendix C.3).
 435

436 We present the resulting estimation of our bound in Table 1, for different learning rates and batch
 437 sizes. A consistent pattern can be observed: the estimated bounds are typically close to an order
 438



432
433
434
435
436
437
438
439
440
441
442
443
444
445
446
447
448
449
450
451
452
453
454
455
456
457
458
459
460
461
462
463
464
465
466
467
468
469
470
471
472
473
474
475
476
477
478
479
480
481
482
483
484
485
Figure 2: Variation of E^1 with sample size n for the model **ViT**. Pearson correlation coefficients r are reported for each subgroup.

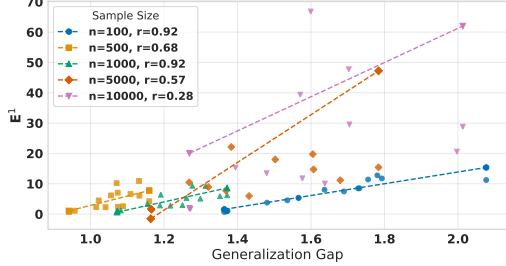


Figure 3: Variation of E^1 with sample size n for the model **GraphSage**. Pearson correlation coefficients r are reported for each subgroup.

of magnitude larger than the actual worst-case generalization error. However, in most experimental settings, the estimated bounds remain below 100% accuracy, hence, provide meaningful guarantees. We also find that the stability parameter β_n varies with the hyperparameters (η, b) and, therefore, encodes the impact of the learning algorithm on generalization error. Moreover, the estimated β_n captures the generalization behavior: specifically, $G_S(\mathcal{W}_{S,U})$ tends to decrease as β_n becomes smaller, a trend that holds for both ViT and GraphSage.

To the best of our knowledge, we are the first to *fully* estimate a bound on the worst-case error, thereby providing a stronger guarantee than in prior work. In contrast, previous studies focused on bounds for a single weight vector and similarly reported discrepancies of one to two orders of magnitude between the estimated bound and the actual error Chen et al. (2018); Li et al. (2019); Dupuis et al. (2023); Harel et al. (2025). This sug-

Table 1: Comparison of ViT and GraphSage across different learning rates (η) and batch sizes (b) . We report β_n , $G_S(\mathcal{W}_{S,U})$, and the resulting bound. We use the 0-1 loss.

Model	η	b	$10^4 \cdot \beta_n$	$10^2 \cdot G_S(\mathcal{W}_{S,U})$	$10^2 \cdot \text{Bound}$
ViT	10^{-4}	64	4.72 ± 0.52	10.24 ± 0.36	104.43
	10^{-4}	128	5.52 ± 0.67	12.84 ± 0.55	105.24
	10^{-5}	64	2.16 ± 0.36	7.16 ± 0.33	68.47
	10^{-5}	128	2.24 ± 0.22	6.36 ± 0.33	68.67
GraphSage	10^{-4}	64	2.56 ± 0.36	5.48 ± 0.36	75.63
	10^{-4}	128	2.64 ± 0.22	5.20 ± 0.40	75.79
	10^{-5}	64	0.64 ± 0.22	4.60 ± 0.14	47.79
	10^{-5}	128	0.80 ± 0.00	4.84 ± 0.17	48.59

gests that our worst-case generalization bounds are reasonable tight. Moreover, the fact that smaller estimated generalization gaps are consistently associated with smaller stability parameters and, therefore, smaller bounds, shows that the bounds adapt meaningfully to model performance.

Interplay between Stability and $C(\mathcal{W}_{S,U})$. In Figure 2 and 3, we observe that the sensitivity of $E^1(\mathcal{W}_{S,U})$ with respect to the generalization gap (i.e., the slope of the affine regression of $E^1(\mathcal{W}_{S,U})$ by the value of $G_S(\mathcal{W}_{S,U})$) increases when n gets larger, which is what is predicted by our theory. Indeed, Theorem 4.4 assert that $\log E^1(\mathcal{W}_{S,U})$ should be (approximately) of order at least $\beta_n^{-1/3} G_S(\mathcal{W}_{S,U})$, which amounts to $n^{1/3} G_S(\mathcal{W}_{S,U})$ in the event that $\beta_n = \Theta(1/n)$. Therefore, our experimental results strongly support Theorem 4.4. Together, these observations unveil a strong coupling between stability and the topological complexity of the training trajectories. Moreover, the topological complexities increase for large n and therefore become more relevant to the bound. The empirically observed coupling is supported by the theoretical results of Section 3, through the product of the stability parameter β_n and the topological complexities. Finally, we observe that the reported Pearson correlations are lower for bigger n , especially for the GraphSage experiment. We believe that it could be due to the fact that reaching local minima is harder when n increases, which can decrease the correlation between the topological complexities and the generalization error, as it was already reported in (Birdal et al., 2021; Andreeva et al., 2024).

6 CONCLUDING REMARKS

In this work, we present a new framework for obtaining worst-case generalization bounds over data-dependent random sets. This framework is based on a new concept of *random set stability*, which we demonstrate holds for practically used algorithms, and is related to classical stability notions. We then bound the worst-case generalization error by the (weighted) sum of the random set stability parameter and a Rademacher complexity term. We present several applications of our new techniques by recovering classical generalization bounds and proving mutual information-free versions

486 of existing fractal and topological bounds, which makes them for the first time fully computable.
 487 We supported our theory through a series of experiments conducted in practically relevant settings.
 488

489 **Limitations & future work.** Despite providing the first mutual information-free topological and
 490 fractal bounds, our main results have two main disadvantages: *(i)* we only provide expected bounds,
 491 and *(ii)* our framework only allows for Euclidean-based topological complexities, and we typically
 492 do not cover the case of the data-dependent pseudometric introduced by Dupuis et al. (2023). [Other
 493 methods to remove information-theoretic terms exist in the literature](#). For instance, Neu et al. (2021)
 494 added Gaussian noise to the algorithm output in their study of the generalization error of SGD.
 495 Extending such a technique to the random set setting is a promising direction for future works.
 496 Finally, while our paper extends uniform stability to random sets, we believe that other notions of
 497 stability, like the one of Lei & Ying (2020) could be extended to our random set setting and might
 498 lead to better generalization bounds under specific assumptions.

499 **Ethics statement.** This work adheres to the ICLR Code of Ethics, ensuring responsible use of pub-
 500 licly available datasets and maintaining full transparency in experimental design and reporting. The
 501 study complies with ethical guidelines on the integrity of research and considers possible social im-
 502 pacts. We have not used data collected on human subjects. In order to minimize carbon emissions,
 503 we utilized high-end GPUs only when they are necessary to train our large models. Since contribu-
 504 tions are primarily theoretical, the focus is on advancing our understanding of the theory of artificial
 505 intelligence rather than targeting specific applications that may have direct societal impacts.

506 **Reproducibility Statement.** All data sets used in this work are referenced and publicly accessible.
 507 The experimental configurations and computational environment are outlined in detail within the
 508 main text and the appendix. The original code, accompanied by instructions, is included in the
 509 Supplementary Material. Lastly, all random seeds are provided to facilitate precise reproducibility.
 510 We plan to make our implementation available upon publication.

511 BIBLIOGRAPHY

513 Henry Adams, Manuchehr Aminian, Elin Farnell, Michael Kirby, Joshua Mirth, Rachel Neville,
 514 Chris Peterson, and Clayton Shonkwiler. A fractal dimension for measures via persistent homol-
 515 ogy. In *Topological Data Analysis: The Abel Symposium 2018*, pp. 1–31. Springer, 2020.

517 Rayna Andreeva, Katharina Limbeck, Bastian Rieck, and Rik Sarkar. Metric space magnitude and
 518 generalisation in neural networks. In *Topological, Algebraic and Geometric Learning Workshops*
 519 2023, pp. 242–253. PMLR, 2023.

520 Rayna Andreeva, Benjamin Dupuis, Rik Sarkar, Tolga Birdal, and Umut Simsekli. Topological
 521 generalization bounds for discrete-time stochastic optimization algorithms. *Advances in Neural*
 522 *Information Processing Systems*, 37:4765–4818, 2024.

523 Peter Bartlett and Shahar Mendelson. Rademacher and Gaussian Complexities: Risk Bounds and
 524 Structural Results. *Journal of Machine Learning Research*, 2002.

526 Raef Bassily, Vitaly Feldman, Cristóbal Guzmán, and Kunal Talwar. Stability of stochastic gradient
 527 descent on nonsmooth convex losses. In H. Larochelle, M. Ranzato, R. Hadsell, M.F. Balcan, and
 528 H. Lin (eds.), *Advances in Neural Information Processing Systems*, volume 33, pp. 4381–4391.
 529 Curran Associates, Inc., 2020. URL https://proceedings.neurips.cc/paper_files/paper/2020/file/2e2c4bf7ceaa4712a72dd5ee136dc9a8-Paper.pdf.

531 Tolga Birdal, Aaron Lou, Leonidas J Guibas, and Umut Simsekli. Intrinsic dimension, persistent
 532 homology and generalization in neural networks. *Advances in Neural Information Processing*
 533 *Systems*, 34:6776–6789, 2021.

535 Vladimir Bogachev. *Measure theory*. Springer, 2007.

536 Jean-Daniel Boissonnat, Frédéric Chazal, and Mariette Yvinec. *Geometric and topological infer-
 537 ence*, volume 57. Cambridge University Press, 2018.

538 Olivier Bousquet and André Elisseeff. Stability and generalization. *J. Mach. Learn. Res.*, pp. 499–
 539 526, 2002.

540 Olivier Bousquet, Yegor Klochkov, and Nikita Zhivotovskiy. Sharper bounds for uniformly sta-
 541 ble algorithms. In Jacob Abernethy and Shivani Agarwal (eds.), *Proceedings of Thirty Third*
 542 *Conference on Learning Theory*, volume 125 of *Proceedings of Machine Learning Research*, pp.
 543 610–626. PMLR, 09–12 Jul 2020.

544 Yuansi Chen, Chi Jin, and Bin Yu. Stability and convergence trade-off of iterative optimization
 545 algorithms. *arXiv preprint arXiv:1804.01619*, 2018.

546 Alexey Dosovitskiy, Lucas Beyer, Alexander Kolesnikov, Dirk Weissenborn, Xiaohua Zhai, Thomas
 547 Unterthiner, Mostafa Dehghani, Matthias Minderer, Georg Heigold, Sylvain Gelly, Jakob Uszkoreit,
 548 and Neil Houlsby. An image is worth 16x16 words: Transformers for image recogni-
 549 tion at scale. In *International Conference on Learning Representations*, 2021. URL <https://openreview.net/forum?id=YicbFdNTTy>.

550 Benjamin Dupuis and Paul Viallard. From mutual information to expected dynamics: New general-
 551 ization bounds for heavy-tailed sgd, 2023. URL <https://arxiv.org/abs/2312.00427>.

552 Benjamin Dupuis, George Deligiannidis, and Umut Simsekli. Generalization bounds using data-
 553 dependent fractal dimensions. In *International conference on machine learning*, pp. 8922–8968.
 554 PMLR, 2023.

555 Benjamin Dupuis, Paul Viallard, George Deligiannidis, and Umut Simsekli. Uniform generalization
 556 bounds on data-dependent hypothesis sets via PAC-bayesian theory on random sets. *Journal of*
 557 *Machine Learning Research*, 25(409):1–55, 2024.

558 Kenneth Falconer. *Fractal geometry: mathematical foundations and applications*. John Wiley &
 559 Sons, 2013.

560 Vitaly Feldman and Jan Vondrak. High probability generalization bounds for uniformly stable algo-
 561 rithms with nearly optimal rate. In Alina Beygelzimer and Daniel Hsu (eds.), *Proceedings of the*
 562 *Thirty-Second Conference on Learning Theory*, volume 99 of *Proceedings of Machine Learning*
 563 *Research*, pp. 1270–1279. PMLR, 25–28 Jun 2019.

564 Dylan J Foster, Spencer Greenberg, Satyen Kale, Haipeng Luo, Mehryar Mohri, and Karthik Srid-
 565 haran. Hypothesis set stability and generalization. *Advances in Neural Information Processing*
 566 *Systems*, 32, 2019.

567 Jingwen Fu, Zhizheng Zhang, Dacheng Yin, Yan Lu, and Nanning Zheng. Learning trajectories are
 568 generalization indicators. *Advances in Neural Information Processing Systems*, 36, 2024.

569 Will Hamilton, Zhitao Ying, and Jure Leskovec. Inductive representation learning on large graphs.
 570 In *Advances in neural information processing systems*, pp. 1024–1034, 2017.

571 Moritz Hardt, Ben Recht, and Yoram Singer. Train faster, generalize better: Stability of stochastic
 572 gradient descent. In *International conference on machine learning*, pp. 1225–1234. PMLR, 2016.

573 Itamar Harel, Yonathan Wolanowsky, Gal Vardi, Nathan Srebro, and Daniel Soudry. Temperature is
 574 all you need for generalization in langevin dynamics and other markov processes. *arXiv preprint*
 575 *arXiv:2505.19087*, 2025.

576 Liam Hodgkinson, Umut Simsekli, Rajiv Khanna, and Michael Mahoney. Generalization bounds
 577 using lower tail exponents in stochastic optimizers. In *International Conference on Machine*
 578 *Learning*, pp. 8774–8795. PMLR, 2022.

579 Diederik P Kingma and Jimmy Ba. Adam: A method for stochastic optimization. *arXiv preprint*
 580 *arXiv:1412.6980*, 2014.

581 Gady Kozma, Zvi Lotker, and Gideon Stupp. The minimal spanning tree and the upper box dimen-
 582 sion. *Proceedings of the American Mathematical Society*, 134(4):1183–1187, 2006.

583 Yunwen Lei and Yiming Ying. Fine-grained analysis of stability and generalization for stochastic
 584 gradient descent. In Hal Daumé III and Aarti Singh (eds.), *Proceedings of the 37th International*
 585 *Conference on Machine Learning*, volume 119 of *Proceedings of Machine Learning Research*,
 586 pp. 5809–5819. PMLR, 13–18 Jul 2020.

594 Tom Leinster. The magnitude of metric spaces. *Documenta Mathematica*, 18:857–905, 2013.
 595

596 Jian Li, Xuanyuan Luo, and Mingda Qiao. On generalization error bounds of noisy gradient methods
 597 for non-convex learning. *arXiv preprint arXiv:1902.00621*, 2019.

598 Pertti Mattila. *Geometry of sets and measures in Euclidean spaces: fractals and rectifiability*, vol-
 599 ume 44. Cambridge university press, 1999.
 600

601 Mark W Meckes. Positive definite metric spaces. *Positivity*, 17(3):733–757, 2013.
 602

603 Mark W Meckes. Magnitude, diversity, capacities, and dimensions of metric spaces. *Potential
 604 Analysis*, 42:549–572, 2015.

605 Ilya Molchanov. *Theory of Random Sets*. Number 87 in Probability Theory and Stochastic Modeling.
 606 Springer, second edition edition, 2017.
 607

608 Federico Monti, Davide Boscaini, Jonathan Masci, Emanuele Rodolà, Jan Svoboda, and Michael M
 609 Bronstein. Geometric deep learning on graphs and manifolds using mixture model cnns. In
 610 *Proceedings of the IEEE conference on computer vision and pattern recognition*, pp. 5115–5124,
 611 2017.

612 Gergely Neu, Gintare Karolina Dziugaite, Mahdi Haghifam, and Daniel M. Roy. Information-
 613 theoretic generalization bounds for stochastic gradient descent. In Mikhail Belkin and Samory
 614 Kpotufe (eds.), *Proceedings of Thirty Fourth Conference on Learning Theory*, volume 134 of
 615 *Proceedings of Machine Learning Research*, pp. 3526–3545. PMLR, 15–19 Aug 2021.
 616

617 Ankit Pensia, Varun Jog, and Po-Ling Loh. Generalization Error Bounds for Noisy, Iterative Algo-
 618 rithms. *IEEE International Symposium on Information Theory (ISIT)*, 2018.

619 Julián Burella Pérez, Sydney Hauke, Umberto Lupo, Matteo Caorsi, and Alberto Dassatti. giotto-
 620 ph: a python library for high-performance computation of persistent homology of veltoris-rips
 621 filtrations. *arXiv preprint arXiv:2107.05412*, 2021.

622 Sarah Sachs, Tim van Erven, Liam Hodgkinson, Rajiv Khanna, and Umut Şimşekli. Generalization
 623 guarantees via algorithm-dependent rademacher complexity. In *The Thirty Sixth Annual Confer-
 624 ence on Learning Theory*, pp. 4863–4880. PMLR, 2023.

625 Shilan Salim. *The q -spread dimension and the maximum diversity of square grid metric spaces*.
 626 PhD thesis, University of Sheffield, 2021.

627 Benjamin Schweinhart. Fractal dimension and the persistent homology of random geometric com-
 628 plexes. *Advances in Mathematics*, 372:107291, 2020. Publisher: Elsevier.

629 Shai Shalev-Shwartz and Shai Ben-David. *Understanding machine learning: From theory to algo-
 630 rithms*. Cambridge university press, 2014.

631 Umut Simsekli, Ozan Sener, George Deligiannidis, and Murat A Erdogdu. Hausdorff dimension,
 632 heavy tails, and generalization in neural networks. *Advances in Neural Information Processing
 633 Systems*, 33:5138–5151, 2020.

634 Thomas Steinke and Lydia Zakynthinou. Reasoning About Generalization via Conditional Mutual
 635 Information. In *Conference on Learning Theory (COLT)*, 2020.

636 Charlie Tan, Inés García-Redondo, Qiquan Wang, Michael M. Bronstein, and Anthea Monod. On the
 637 limitations of fractal dimension as a measure of generalization. In *Proceedings of the 38th Con-
 638 ference on Neural Information Processing Systems (NeurIPS)*, 2024. URL https://papers.nips.cc/paper_files/paper/2024/hash/<paper_id>-Abstract.html.

639 Vladimir Vapnik and Vlaminir Vapnik. Statistical learning theory wiley. *New York*, 1(624):2, 1998.

640 Aolin Xu and Maxim Raginsky. Information-Theoretic Analysis of Generalization Capability of
 641 Learning Algorithms. *Advances in Neural Information Processing Systems (NIPS 2017)*, 2017.

648 Jing Xu, Jiaye Teng, Yang Yuan, and Andrew Yao. Towards data-algorithm dependent general-
649 ization: a case study on overparameterized linear regression. *Advances in Neural Information
650 Processing Systems*, 36, 2024.

651

652 Chiyuan Zhang, Samy Bengio, Moritz Hardt, Benjamin Recht, and Oriol Vinyals. Understanding
653 deep learning requires rethinking generalization. *ICLR*, 2017.

654

655 Chiyuan Zhang, Samy Bengio, Moritz Hardt, Benjamin Recht, and Oriol Vinyals. Understanding
656 deep learning (still) requires rethinking generalization. *Communications of the ACM*, 64(3):107–
657 115, 2021. Publisher: ACM New York, NY, USA.

658

659 Lingjiong Zhu, Mert Gurbuzbalaban, Anant Raj, and Umut Simsekli. Uniform-in-time wasserstein
660 stability bounds for (noisy) stochastic gradient descent. In *Thirty-seventh Conference on Neu-
661 ral Information Processing Systems*, 2023. URL <https://openreview.net/forum?id=8fLatmFQgF>.

662

663

664

665

666

667

668

669

670

671

672

673

674

675

676

677

678

679

680

681

682

683

684

685

686

687

688

689

690

691

692

693

694

695

696

697

698

699

700

701

APPENDICES

We now provide additional technical details and proofs that are omitted from the main write-up. Further, we provide additional technical and empirical results. The appendix is thus organized in the following way:

- **Appendix A** provides supplementary technical background.
- **Appendix B** contains the omitted proofs of all our theoretical results.
- **Appendix C** details the experimental setup and procedures required for reproducibility.
- **Appendix D** presents additional empirical results.

A ADDITIONAL TECHNICAL BACKGROUND

In this section, we provide the relevant definitions as well as the technical background for our results.

A.1 RADEMACHER COMPLEXITY

Recent advances on topological generalization bounds are based on a data-dependent Rademacher complexity, leveraging PAC-Bayesian theory on random sets Dupuis et al. (2024). In our stability-based approach, the Rademacher complexity also plays a central role. We define the standard Rademacher complexity Shalev-Shwartz & Ben-David (2014); Bartlett & Mendelson (2002) as:

Definition A.1. Let $\mathcal{W} \subset \mathbb{R}^d$, $S \in \mathcal{Z}^n$, and $\epsilon := (\epsilon_1, \dots, \epsilon_n) \sim \mathcal{U}(\{-1, 1\})^{\otimes n}$ be i.i.d Rademacher random variables (i.e., centered Bernoulli variables). Let $\ell : \mathcal{W} \times \mathcal{Z} \rightarrow \mathbb{R}_+$ be a loss function. We define the Rademacher complexity of \mathcal{W} (relative to ℓ) as:

$$\mathbf{Rad}_S(\mathcal{W}) := \mathbb{E}_\epsilon \left[\sup_{w \in \mathcal{W}} \frac{1}{n} \sum_{i=1}^n \epsilon_i \ell(w, z_i) \right].$$

Intuitively, the Rademacher complexity measures the ability of a model to fit random labels. Using this definition, we now establish our main result.

A.2 COVERING AND PACKING NUMBERS

In this section, we provide definitions of covering and packing numbers. These quantities have long been central in learning theory, particularly in the context of classical covering-based arguments for Rademacher complexity Shalev-Shwartz & Ben-David (2014); Bartlett & Mendelson (2002).

Definition A.2 (Covering number). Let (\mathcal{W}, ρ) be a metric space with $\mathcal{W} \subset \mathbb{R}^d$ of finite diameter, and let $\delta > 0$. The *covering number* $N_\delta(\mathcal{W})$ is the smallest integer $K \in \mathbb{N}^*$ such that there exist points $x_1, \dots, x_K \in \mathcal{W}$ satisfying

$$\mathcal{W} \subset \bigcup_{k=1}^K B_\rho(x_k, \delta),$$

where $B_\rho(x, \delta)$ denotes the open ball of radius δ centered at x with respect to the metric ρ .

In this definition, we take the centers (x_1, \dots, x_K) of the covering to be in \mathcal{W} . This allows us to leverage the "local" Lipschitz continuity assumption defined in Assumption 4.1. This definition does not lose any generality compared to taking the points in \mathbb{R}^d . In particular, both definitions yield the same fractal dimensions (Falconer, 2013).

Definition A.3 (Packing number). Let (\mathcal{W}, ρ) be a metric space and $\delta > 0$. The *packing number* $P_\delta^\rho(\mathcal{W})$ is the cardinality of a maximal set of points in \mathcal{W} such that the closed balls of radius δ centered at these points are pairwise disjoint.

756 A.3 INTRINSIC DIMENSIONS
757

758 In this section, we focus on the upper box-counting dimension (also known as the upper Minkowski
759 dimension), one of the most widely used notions of fractal dimension Falconer (2013); Mattila
760 (1999). This notion has also found applications in machine learning, for instance in the works of
761 Simsekli et al. (2020); Dupuis et al. (2023).

762 **Definition A.4** (Upper box-counting dimension). Let (\mathcal{W}, ρ) be a metric space of finite diameter
763 and let $(|N_\delta(\mathcal{W})|)_{\delta>0}$ denote the covering numbers introduced in Definition A.2. The upper box-
764 counting dimension is defined by:

$$765 \overline{\dim}_{\text{B}}(\mathcal{W}) := \limsup_{\delta \rightarrow 0} \frac{\log |N_\delta(\mathcal{W})|}{\log(1/\delta)}.$$

768 We refer the reader to (Falconer, 2013) for more technical background on this notion.

769 **Remark A.1.** It has been shown in Kozma et al. (2006); Schweinhart (2020) that, for any compact
770 metric space, several notions of dimension coincide with the well-known upper box-counting di-
771 mension (see Definition A.4). In particular, the celebrated *persistent homology dimension* Adams
772 et al. (2020) has been connected to generalization Birdal et al. (2021) and has also been studied
773 empirically in various works Andreeva et al. (2024); Tan et al. (2024).

775 A.4 TOPOLOGICAL COMPLEXITIES
776

777 In this section, we define the topological quantities appearing in Theorem 4.4.

778 **α -weighted lifetime sum (\mathbf{E}^α).** The weighted lifetime sums is a central notion in the study of
779 persistent homology, a subfield of topological data analysis (TDA). The interested reader may find a
780 full exposition of these notions in (Boissonnat et al., 2018; Schweinhart, 2020; Kozma et al., 2006).
781 There exist several equivalent definitions the weighted lifetime sums of degree 0, see (Andreeva
782 et al., 2024) for a concise review of these definitions in the context of machine learning.

783 In this section, we present an intuitive approach to the weighted lifetime sum, which we also restrict
784 to finite subsets of \mathbb{R}^d and to homology of dimension 0. Note that this is a simplified, non-standard
785 (though equivalent) definition of PH^0 .

786 **Definition A.5** (Persistent homology of degree 0 PH^0). Let $\mathcal{W} \subset \mathbb{R}^d$ be a finite set with cardinality
787 N , endowed with the Euclidean metric. For each $t \geq 0$ (which is often referred to as a “time”
788 variable in the TDA literature), we construct an undirected graph G_t with edges given by

$$790 \forall x, y \in \mathcal{W}, \quad \{x, y\} \in G_t \iff \rho(x, y) \leq t.$$

791 There exists a finite sequence of times $0 < t_1 < \dots < t_k < +\infty$ such that the number of connected
792 components in G_{t_i} changes compared to G_t for $t < t_i$. Let c_i denote the number of connected
793 components in G_{t_i} . By convention, set $c_0 = N$ and $t_0 = 0$, and define $n_i := c_i - c_{i-1}$. Then PH^0
794 is defined as the multi-set,

$$795 \text{PH}^0(\mathcal{W}) := \left\{ \underbrace{\{t_1, \dots, t_1\}}_{n_1 \text{ times}}, \underbrace{\{t_2, \dots, t_k\}}_{n_k \text{ times}}, \dots \right\},$$

796 where the notation $\{\cdot\}$ denotes a multi-set.

797 **Remark A.2.** The construction of the graph above consists in looking at the 1-dimensional simplices
798 of the Rips complex associated with \mathcal{W} , see (Boissonnat et al., 2018, Chapter 2).

800 We now use PH^0 to define the key quantities in our work, in particular the α -weighted sum \mathbf{E}_ρ^α .

801 **Definition A.6** (α -weighted lifetime sums). Let $\mathcal{W} \subset \mathbb{R}^d$ be a finite subsets of \mathbb{R}^d , endowed with
802 the Euclidean metric. For $\alpha \geq 0$, the α -weighted lifetime sum of \mathcal{W} is defined as

$$806 \mathbf{E}^\alpha(\mathcal{W}) := \sum_{t \in \text{PH}^0(\mathcal{W})} t^\alpha,$$

807 where PH^0 denotes the set of lifetimes of the 0-dimensional persistent homology intervals of \mathcal{W} , or,
808 equivalently, the above definition.

Magnitude and positive magnitude. Magnitude is another known topological invariant used in TDA, it was introduced by Leinster (2013). In the context of machine learning, it has been used in particular by Andreeva et al. (2023) to analyze the generalization error of neural networks.

A detailed account of this theory can be found in (Meckes, 2013; 2015). In this paragraph, we restrict ourselves to a particular case, that is enough for our purpose. In particular, we only define these notions for finite sets, but all our theoretical results can be seamlessly extended to compact subsets of \mathbb{R}^d (see (Andreeva et al., 2024, Remark B.15)).

In all this paragraph, we fix a finite set $\mathcal{W} \subset \mathbb{R}^d$. The key notion behind both magnitude and positive magnitude is that of a weighting of \mathcal{W} , which is defined below.

Definition A.7 (Weighting). Let $\lambda > 0$. A λ -weighting of \mathcal{W} is a vector $\beta_\lambda \in \mathbb{R}^{\mathcal{W}}$ such that:

$$\forall a \in \mathcal{W}, \sum_{b \in \mathcal{W}} e^{-\lambda \|a-b\|} \beta_\lambda(b) = 1.$$

The existence of such a weighting has been shown by Leinster (2013).

We can now define the magnitude of \mathcal{W} .

Definition A.8 (Magnitude, (Leinster, 2013)). With the notations of Definition A.7, the magnitude function of \mathcal{W} is defined as:

$$(0, +\infty) \ni \lambda \longmapsto \mathbf{Mag}(\lambda \cdot \mathcal{W}) := \sum_{a \in \mathcal{W}} \beta_\lambda(a).$$

Recently, Andreeva et al. (2024) demonstrated that by slightly adapting the definition of magnitude, one obtains an object that is naturally related to the Rademacher complexity (Definition A.1), hence, relating it to learning theory. Therefore, they introduced the notion of *positive magnitude*, which we recall below.

Definition A.9 (Positive magnitude, (Andreeva et al., 2024)). With the notations of Definition A.7, the *positive* magnitude function of \mathcal{W} is defined as:

$$(0, +\infty) \ni \lambda \longmapsto \mathbf{PMag}(\lambda \cdot \mathcal{W}) := \sum_{a \in \mathcal{W}} (\beta_\lambda)_+(a),$$

where $x_+ := \max(x, 0)$.

B OMITTED PROOFS

In this section, we present the omitted proofs in full detail. We also present a few additional technical results that are useful for our proofs and may be of independent interest.

B.1 PROOF OF COROLLARY 3.3

We give below the proof of Corollary 3.3, which provides a random set stability assumption for projected SGD, in smooth and Lipschitz continuous settings.

Corollary 3.3. Suppose that, for all z , $\ell(\cdot, z)$ is L -Lipschitz, $\nabla \ell(\cdot, z)$ is G -Lipschitz, and that $\eta_k \leq c/k$ for some $c < 1/G$. Then, \mathcal{A}_{SGD} is random-set-stable with parameter

$$\beta_n = \frac{4LR}{n-1} \left(\frac{L}{GR} \right)^{1/Gc+1} \sum_{1 \leq k \leq T} k^{\frac{Gc}{Gc+1}}.$$

Proof. To show the trajectory-stability of SGD, we will first show that it is argument-stable in the sense of Definition 2.1, then we will use Lemma 3.2 to establish random set stability.

To prove the argument stability, we almost exactly follow the steps in (Hardt et al., 2016, Theorem 3.12). Let us consider a neighboring dataset $S' = (z'_1, \dots, z'_n) \in \mathcal{Z}^n$ that differs from S by one element, i.e., $z_i = z'_i$ except one element. Consider the SGD recursion on S' :

$$w'_{k+1} = \Pi_R \left[w'_k - \eta_k \nabla \ell(w'_k, z'_{i_{k+1}}) \right].$$

864 Since most of S and S' coincide, at the first iterations it is highly likely that w_k and w'_k will be
 865 identical, since they will pick the same data points. Let us denote the random variable $\kappa \geq 1$ that is
 866 the first time $z_{i_\kappa} \neq z'_{i_\kappa}$. Consider $K \in \mathbb{N}$ with $1 \leq K \leq T$. By using this construction, we have:
 867

$$868 \mathbb{E}_U [\|w_K - w'_K\|] = \mathbb{E}_U [\|w_K - w'_K\| \mathbb{1}_{\kappa \leq t_0}] + \mathbb{E}_U [\|w_K - w'_K\| \mathbb{1}_{\kappa > t_0}].$$

869 We now focus on the first term in the right-hand-side of the above equation:

$$\begin{aligned} 870 \mathbb{E}_U [\|w_K - w'_K\|] &\leq \mathbb{E}_U [(\|w_K\| + \|w'_K\|) \mathbb{1}_{\kappa \leq t_0}] \\ 871 &\leq 2R \mathbb{P}(\kappa \leq t_0) \\ 872 &= \frac{2Rt_0}{n}. \end{aligned} \tag{9}$$

875 The second parameter is upper-bounded in the proof of (Hardt et al., 2016, Theorem 3.12) (adapted
 876 to our setting by noting that the projection on the ball is 1-Lipschitz), which reads as follows:

$$877 \mathbb{E}_U [\|w_K - w'_K\| \mathbb{1}_{\kappa > t_0}] \leq \frac{2L}{G(n-1)} \left(\frac{K}{t_0} \right)^{G_c}.$$

880 By combining these two estimates, we obtain:

$$881 \mathbb{E}_U [\|w_K - w'_K\|] \leq \frac{2Rt_0}{n} + \frac{2L}{G(n-1)} \left(\frac{K}{t_0} \right)^{G_c}.$$

884 Choosing

$$886 t_0 = \left(\frac{L}{GR} \right)^{\frac{1}{G_c+1}} K^{\frac{G_c}{G_c+1}}$$

888 yields

$$\begin{aligned} 890 \mathbb{E}_U [\|w_K - w'_K\|] &\leq \frac{4R}{n-1} \left(\frac{L}{GR} \right)^{\frac{1}{G_c+1}} K^{\frac{G_c}{G_c+1}} \\ 891 &=: \delta_K. \end{aligned}$$

893 Since δ_K is independent of S and S' , this shows that the k -th iterate of SGD is δ_k argument-stable.
 894 Finally, we conclude by Lemma 3.2, that SGD is trajectory-stable with parameter
 895

$$896 \beta_n = L \sum_{k=1}^K \delta_k.$$

897 This concludes the proof. □

901 B.2 A KEY TECHNICAL LEMMA: RADEMACHER BOUND FOR TRAJECTORY-STABLE 902 ALGORITHMS

903 A key technical element of our approach is the following theorem, which presents an expected
 904 Rademacher complexity bound for the worst-case generalization error of trajectory-stable algo-
 905 rithms. Before proceeding to the proof, we recall the following notation for the worst-case gen-
 906 eralization error.

$$908 G_S(\mathcal{W}) := \sup_{w \in \mathcal{W}} (\mathcal{R}(w) - \widehat{\mathcal{R}}_S(w)).$$

910 **Lemma 3.4.** *Let $S \sim \mu_z^{\otimes n}$. Let $J, K \in \mathbb{N}^*$ be such that $n = JK$, and $\tilde{S}_J \sim \mu_z^{\otimes J}$ be independent of
 911 S and \mathcal{U} . Assume that algorithm \mathcal{A} satisfies Assumption 3.1 with parameter $\beta_n > 0$, then:*

$$912 \mathbb{E} [\sup_{w \in \mathcal{W}_{S,U}} (\mathcal{R}(w) - \widehat{\mathcal{R}}_S(w))] \leq 2\mathbb{E} [\mathbf{Rad}_{\tilde{S}_J}(\mathcal{W}_{S,U})] + 2J\beta_n, \tag{8}$$

914 where $\mathbf{Rad}_S(\mathcal{W})$ denotes the Rademacher complexity, whose definition is recalled in Definition A.1.

916 The proof is inspired by the data splitting technique used in (Dupuis et al., 2023, Theorem 3.8),
 917 which we adapt to our purpose of using the trajectory stability assumption to remove the need for
 918 information-theoretic terms.

918 *Proof.* In the following, we consider three independent datasets $S, S', S'' \sim \mu_z^{\otimes n}$, with $S = (z_1, \dots, z_n)$ (and similar notation for S' and S''). Up to a slight change in the constant, we can
919 without loss of generality consider $J, K \in \mathbb{N}^*$ such that $n = JK$. We write the index `set` as a
920 disjoint union as follows:
921

$$923 \quad 924 \quad 925 \quad \{1, \dots, n\} = \coprod_{k=1}^K N_k,$$

926 with for all k , $|N_k| = J$, where \coprod denotes the disjoint union. We also introduce the notation
927 $S_k \in \mathcal{Z}^n$, with:
928

$$929 \quad \forall i \in \{1, \dots, n\}, (S_k)_i = \begin{cases} z'_i, & i \in N_k \\ z_i, & i \notin N_k \end{cases}$$

931 Given two datasets $S_1, S_2 \in \mathcal{Z}^n$, we also consider a measurable mapping $w(\mathcal{W}_{S_1}, S_2)$ (whose
932 existence is satisfied in our setting Molchanov (2017)) such that, almost surely:
933

$$934 \quad \omega(\mathcal{W}_{S_1}, S_2) \in \arg \max_{w \in \mathcal{W}_{S_1}} (\mathcal{R}(w) - \widehat{\mathcal{R}}_{S_2}(w)).$$

936 Recall that $\mathcal{W}_S \in \text{CL}(\mathbb{R}^d)$ (where $\text{CL}(\mathbb{R}^d)$ denotes the closed subsets of \mathbb{R}^d) is a data-dependent
937 random trajectory, which we assume is a random compact set Molchanov (2017). We also denote
938 ρ_S the conditional distribution of \mathcal{W}_S given S . Finally we recall the notation:
939

$$940 \quad G_S(\mathcal{W}_{S,U}) := \sup_{w \in \mathcal{W}_{S,U}} (\mathcal{R}(w) - \widehat{\mathcal{R}}_S(w)).$$

942 We have:
943

$$944 \quad \mathbb{E}[G_S(\mathcal{W}_{S,U})] = \mathbb{E} \left[\mathcal{R}(\omega(\mathcal{W}_{S,U}, S)) - \widehat{\mathcal{R}}_S(\omega(\mathcal{W}_{S,U}, S)) \right] \\ 945 \quad = \frac{1}{n} \mathbb{E} \left[\sum_{k=1}^K \sum_{i \in N_k} (\ell(\omega(\mathcal{W}_{S,U}, S), z''_i) - \ell(\omega(\mathcal{W}_{S,U}, S), z_i)) \right].$$

948 By Assumption 3.1 there exists a measurable function $\omega' : \text{CL}(\mathbb{R}^d) \times \mathcal{Z}^n \rightarrow \mathbb{R}^d$ such that for any
949 $z \in \mathcal{Z}$
950

$$951 \quad \mathbb{E}_U[|\ell(\omega(\mathcal{W}_{S,U}, S), z) - \ell(\omega'(\mathcal{W}_{S,U}, \omega(\mathcal{W}_{S,U}, S)), z)|] \leq J\beta_n.$$

953 We now apply the stability assumption on each term of the sum to get:
954

$$955 \quad \mathbb{E}[G_S(\mathcal{W}_{S,U})] \leq 2J\beta_n + \frac{1}{n} \mathbb{E} \left[\sum_{k=1}^K \sum_{i \in N_k} (\ell(\omega'(\mathcal{W}_{S_k,U}, \omega(\mathcal{W}_{S,U}, S)), z''_i) - \ell(\omega'(\mathcal{W}_{S_k,U}, \omega(\mathcal{W}_{S,U}, S)), z_i)) \right] \\ 956 \quad \leq 2J\beta_n + \frac{1}{K} \mathbb{E} \left[\sum_{k=1}^K \sup_{w \in \mathcal{W}_{S_k,U}} \frac{1}{J} \sum_{i \in N_k} (\ell(w, z''_i) - \ell(w, z_i)) \right] \\ 957 \quad \leq 2J\beta_n + \frac{1}{K} \mathbb{E} \left[\sum_{k=1}^K \sup_{w \in \mathcal{W}_{S,U}} \frac{1}{J} \sum_{i \in N_k} (\ell(w, z''_i) - \ell(w, z'_i)) \right],$$

963 where the last equation follows by linearity of the expectation independence by interchanging z_i and
964 z'_i for all $i \in N_k$. By noting that all the terms inside the first sum have the same distribution, we
965 have:
966

$$967 \quad \mathbb{E}[G_S(\mathcal{W}_{S,U})] \leq 2J\beta_n + \frac{1}{K} \sum_{k=1}^K \mathbb{E} \left[\sup_{w \in \mathcal{W}_{S,U}} \frac{1}{J} \sum_{i \in N_k} (\ell(w, z''_i) - \ell(w, z'_i)) \right] \\ 968 \quad = 2J\beta_n + \mathbb{E} \left[\sup_{w \in \mathcal{W}_{S,U}} \frac{1}{J} \sum_{i \in N_1} (\ell(w, z''_i) - \ell(w, z'_i)) \right],$$

As $\mathcal{W}_{S,U}$ is independent of S' and S'' , we can apply the classical symmetrization argument. More precisely, let $(\epsilon_1, \dots, \epsilon_n) \sim \mathcal{U}(\{-1, 1\})^{\otimes n}$ be i.i.d. Rademacher random variables (i.e., centered Bernoulli random variables), independent from the other random variable. We have:

$$\begin{aligned} \mathbb{E}[G_S(\mathcal{W}_{S,U})] &\leq 2J\beta_n + \mathbb{E}\left[\sup_{w \in \mathcal{W}_{S,U}} \frac{1}{J} \sum_{i \in N_1} \epsilon_i (\ell(w, z''_i) - \ell(w, z'_i))\right] \\ &\leq 2J\beta_n + \mathbb{E}\left[\sup_{w \in \mathcal{W}_{S,U}} \frac{1}{J} \sum_{i \in N_1} \epsilon_i \ell(w, z''_i)\right] + \mathbb{E}\left[\sup_{w \in \mathcal{W}_{S,U}} \frac{1}{J} \sum_{i \in N_1} (-\epsilon_i) \ell(w, z'_i)\right] \\ &= 2J\beta_n + 2\mathbb{E}\left[\sup_{w \in \mathcal{W}_{S,U}} \frac{1}{J} \sum_{i \in N_1} \epsilon_i \ell(w, z'_i)\right]. \end{aligned}$$

Therefore, by denoting $\tilde{S}_J = (z'_i)_{i \in N_1}$, we obtain by definition of the Rademacher complexity that:

$$\mathbb{E}[G_S(\mathcal{W}_{S,U})] \leq 2J\beta_n + 2\mathbb{E}[\mathbf{Rad}_{\tilde{S}_J}(\mathcal{W}_{S,U})],$$

which is the desired result. \square

This result is based on leveraging our stability assumption to enable the use of the classical symmetrization argument Shalev-Shwartz & Ben-David (2014). Compared to previously proposed modified Rademacher complexity bounds, Foster et al. (2019); Sachs et al. (2023), the above theorem has the advantage of directly involving the Rademacher complexity of the data-dependent hypothesis set \mathcal{W}_S , which tightens the bound and makes it significantly more empirically relevant.

Compared to previous studies Foster et al. (2019); Dupuis et al. (2024), a drawback of our bound compared to these studies is that it only holds in expectation. Moreover, while we directly involve the data-dependent trajectory \mathcal{W}_S , our Rademacher $\mathbf{Rad}_{\tilde{S}}(\mathcal{W}_S)$ term uses an independent copy of the dataset, hence, losing some data dependence compared to the term $\mathbf{Rad}_S(\mathcal{W}_S)$ obtained by Dupuis et al. (2024). That being said, we show that our techniques still recover certain topological complexities, at the cost of requiring an additional Lipschitz continuity assumption. The Rademacher complexity term appearing in Lemma 3.4 uses the data-dependent trajectory \mathcal{W}_S and an independent dataset \tilde{S} of size J . Following classical arguments Shalev-Shwartz & Ben-David (2014); Andreeva et al. (2024), we expect this term to behave as $\mathcal{O}(1/\sqrt{J})$, hence, optimizing the value of J yields a bound of order $\mathcal{O}(\beta_n^{1/3})$.

B.3 COVERING BOUNDS

In this section, we present worst-case generalization bounds over data-dependent random sets based on covering numbers, as they have been defined in Definition A.2. These covering bounds serve as a basis to derive some of our other main results, namely, our generalization bounds based on fractal dimension and α -weighted lifetime sums. We believe that these additional contributions are also of independent interest.

The following lemma is a consequence of classical covering argument for Rademacher complexity (Shalev-Shwartz & Ben-David, 2014).

Lemma B.1 (Covering lemma). *Let $\mathcal{W} \subset \mathbb{R}^d$ be a set with finite diameter. We assume that Assumption 4.2 holds and that the loss $\ell(\cdot, z)$ is L -Lipschitz continuous for all $z \in \mathcal{Z}$. Let $m \in \mathbb{N}^*$ and $S \in \mathcal{Z}^m$, we have*

$$\mathbf{Rad}_S(\mathcal{W}) \leq \inf_{\delta > 0} \left(L\delta + B\sqrt{\frac{2 \log |N_\delta(\mathcal{W})|}{m}} \right)$$

The argument is very classical, we reproduce it briefly for the sake of completeness.

Proof. Let $\delta > 0$ and $N := |N_\delta(\mathcal{W})|$ and let (x_1, \dots, x_N) be a minimal δ -cover of \mathcal{W} . By Lipschitz continuity, we have that:

$$\mathbf{Rad}_S(\mathcal{W}) \leq L\delta + \mathbf{Rad}_S(\{x_1, \dots, x_N\}).$$

1026 By Massart's lemma (Shalev-Shwartz & Ben-David, 2014, Lemma 26.8), we have that
 1027

$$1028 \mathbf{Rad}_S(\mathcal{W}) \leq L\delta + B\sqrt{\frac{2\log N}{m}} = L\delta + B\sqrt{\frac{2\log |N_\delta(\mathcal{W})|}{m}}.$$

1029 We conclude by taking the infimum over $\delta > 0$. \square
 1030

1031 To illustrate the power of our framework, we present in the next theorem a data-dependent worst-
 1032 case bounds for stable random sets in terms of covering numbers of $\mathcal{W}_{S,U}$.
 1033

1034 **Theorem B.2.** *Suppose that Assumptions 4.2, 3.1, and 4.1 hold, and that $\mathcal{W}_{S,U}$ is almost surely of
 1035 finite diameter. Without loss of generality, assume that $\beta_n^{-2/3}$ is an integer divisor of n^4 . We have:*
 1036

$$1037 \mathbb{E} \left[\sup_{w \in \mathcal{W}_{S,U}} (\mathcal{R}(w) - \widehat{\mathcal{R}}_S(w)) \right] \leq 2\mathbb{E} \left[\inf_{\delta > 0} \left(\delta L_{S,U} + \beta_n^{1/3} \left(1 + B\sqrt{2\log |N_\delta(\mathcal{W}_{S,U})|} \right) \right) \right],$$

1038 where $|N_\delta(\mathcal{W}_{S,U})|$ is covering number, i.e., the minimum number of balls of radius δ that are nec-
 1039 essary to cover $\mathcal{W}_{S,U}$.
 1040

1041 *Proof.* By Lemma 3.4, we have (recall that G_S has been defined in Equation (4)):
 1042

$$1043 \mathbb{E} [G_S(\mathcal{W}_{S,U})] \leq 2\mathbb{E} [\mathbf{Rad}_{\tilde{S}_J}(\mathcal{W}_{S,U})] + 2J\beta_n,$$

1044 with the notations of Lemma 3.4 for \tilde{S}_J . By Assumption 4.1, for fixed (S, U) the loss $\ell(\cdot, \mathcal{Z})$ is
 1045 L -Lipschitz continuous for all $z \in \mathcal{Z}$. Therefore, we can apply Lemma B.1 to obtain that
 1046

$$1047 \mathbb{E} [G_S(\mathcal{W}_{S,U})] \leq 2\mathbb{E} \left[\inf_{\delta > 0} \left(\delta L_{S,U} + B\sqrt{\frac{2\log |N_\delta(\mathcal{W}_{S,U})|}{J}} \right) \right] + 2J\beta_n,$$

1048 We make the choice $J := \beta_n^{-2/3}$, which we assumed for simplicity is an integer dividing n , so that
 1049 it is a valid choice. This immediately gives the result. \square
 1050

1051 Covering bounds are widely used for worst-case bounds over data-independent hypothesis sets (i.e.,
 1052 Example 1.4) (Shalev-Shwartz & Ben-David, 2014). Theorem B.2 extends these results to data-
 1053 dependent hypothesis sets. Theorem B.2 also improves over the data-dependent covering bounds of
 1054 Dupuis et al. (2024, Corollary 33) by avoiding the use of complicated information-theoretic terms
 1055 and by allowing the Lipschitz constant to be defined only on the data-dependent set $\mathcal{W}_{S,U}$.
 1056

1057 B.4 PROOF OF THEOREM 4.3

1058 We now present the proof of Theorem 4.3. This theorem is based on our key technical lemma
 1059 (Lemma 3.4), the covering lemma (Lemma B.1), and a limit argument that is inspired from previous
 1060 works (Simsekli et al., 2020; Dupuis & Viallard, 2023).
 1061

1062 **Theorem 4.3.** *Suppose that Assumptions 4.2, 3.1, and 4.1 hold, and that $\mathcal{W}_{S,U}$ is a.s. of finite
 1063 diameter. Without loss of generality, assume that $\beta_n^{-2/3}$ is an integer divisor of n . There exists
 1064 $\delta_n > 0$ such that for all $\delta < \delta_n$*

$$1065 \mathbb{E} \left[\sup_{w \in \mathcal{W}_{S,U}} (\mathcal{R}(w) - \widehat{\mathcal{R}}_S(w)) \right] \leq 2\mathbb{E} \left[\frac{B}{n} + \delta L_{S,U} + \beta_n^{1/3} \left(1 + B\sqrt{4\overline{\dim}_B(\mathcal{W}_{S,U}) \log \frac{1}{\delta}} \right) \right],$$

1066 where $\overline{\dim}_B(\mathcal{W}_{S,U})$ is the upper box-counting dimension (Falconer, 2013), which we define in the
 1067 appendix in Definition A.4. We refer to the Appendix B.4 for a discussion of the parameter δ_n .
 1068

1069 *Proof.* Let $(\Omega, \mathcal{F}_U, \mathbb{P}_U)$ denote the probability space to which belongs U , with \mathbb{P}_U denoting the law
 1070 of U . We also denote \mathcal{F} the σ -algebra associated with the data space \mathcal{Z} . As $\mathcal{W}_{S,U}$ is almost-surely
 1071

1072 ⁴Not making this assumption would only lead to minor changes in the bound
 1073

of finite diameter, by definition of the upper box-counting dimension, we have $\mu_z^{\otimes n} \otimes \mathbb{P}_U$ -almost surely that:

$$\overline{\dim}_B(\mathcal{W}_{S,U}) := \limsup_{\delta \rightarrow 0} \frac{\log |N_\delta(\mathcal{W}_{S,U})|}{\log(1/\delta)} = \lim_{\delta \rightarrow 0} \sup_{0 < r < \delta} \frac{\log |N_r(\mathcal{W}_{S,U})|}{\log(1/r)} =: \lim_{\delta \rightarrow 0} f_\delta(\mathcal{W}_{S,U}).$$

Let $(\delta_k)_{k \geq 0}$ be a decreasing positive sequence in $(0, 1)$ with $\delta_k \rightarrow 0$. Let also $\gamma > 0$. By Egoroff's theorem (Bogachev, 2007), there exists a set $\Omega_\gamma \in \mathcal{F}^{\otimes n} \otimes \mathcal{F}_U$ such that $\mu_z^{\otimes n} \otimes \mathbb{P}_U(\Omega_\gamma) \geq 1 - \gamma$, and such that the convergence of $\log f_{\delta_k}(\mathcal{W}_{S,U}) \rightarrow_k \log \overline{\dim}_B(\mathcal{W}_{S,U})$ is uniform on Ω_γ . Therefore, there exists $k_{n,\gamma} > 0$ such that for all $k \geq k_{n,\gamma}$, we have for $(S, U) \in \Omega_\gamma$

$$\log f_{\delta_k}(\mathcal{W}_{S,U}) \leq \log \overline{\dim}_B(\mathcal{W}_{S,U}) + \log 2.$$

Therefore, for all $0 < \delta < \delta_k$, we have by taking the exponential that for $(S, U) \in \Omega_\gamma$:

$$\log |N_\delta(\mathcal{W}_{S,U})| \leq 2 \log(1/\delta) \overline{\dim}_B(\mathcal{W}_{S,U}).$$

Now we use Lemma 3.4 to get that for all J we have

$$\begin{aligned} \mathbb{E}[G_S(\mathcal{W}_{S,U})] &\leq 2\beta_n J + 2\mathbb{E}_{S,U,\tilde{S}}[\mathbf{Rad}_{\tilde{S}_J}(\mathcal{W}_{S,U})] \\ &\leq 2\beta_n J + 2B\mathbb{E}_{S,U,\tilde{S}}[\mathbf{1}_{\Omega_\gamma}(S, U)] + 2\mathbb{E}_{S,U,\tilde{S}}[\mathbf{1}_{\Omega_\gamma}(S, U)\mathbf{Rad}_{\tilde{S}_J}(\mathcal{W}_{S,U})] \\ &\leq 2\beta_n J + 2B\gamma + 2\mathbb{E}_{S,U,\tilde{S}}[\mathbf{1}_{\Omega_\gamma}(S, U)\mathbf{Rad}_{\tilde{S}_J}(\mathcal{W}_{S,U})]. \end{aligned}$$

We make the choice $J := \beta_n^{-2/3}$, which we assumed for simplicity is an integer dividing n , so that it is a valid choice. We conclude the proof by Lemma B.1 and setting $\gamma := 1/n$ and $\delta_n := k_{n,1/n}$. \square

Remark B.1. The careful reader might notice that the proof above requires some measure-theoretic conditions to hold, in particular, the measurability of the mappings $(S, U) \mapsto \mathbf{Rad}_S(\mathcal{W}_{S,U})$ and $(S, U) \mapsto |N_\delta(\mathcal{W}_{S,U})|$. These aspects have been extensively studied in existing works on covering / fractal bounds on random sets (Dupuis et al., 2023; 2024). In our paper, we implicitly assume these conditions to be satisfied for the sake of simplicity, and refer to these works for more details. This choice is justified as our main application regards finite trajectories (Example 1.1), where all this conditions are satisfied.

Remark B.2. The parameter δ_n appearing in the statement of Theorem 4.3 might seem intriguing. It can be seen from the proof that this parameters quantifies the uniformity in n of the limit defining the upper box-counting dimension (i.e., if this convergence is uniform in n , then δ is independent of n). Such a parameter already appears in (Dupuis et al., 2023) in a similar context and it was shown in (Dupuis et al., 2024) that δ can be made independent of n under a convergence assumption of the random sets distributions. We refer to these works for further details.

B.5 PROOF OF THEOREM 4.4

Before presenting the proof of Theorem 4.4, we present two technical lemma, whose proof can be found in Andreeva et al. (2024). The first lemma relates the Rademacher complexity to the α -weighted lifetime sums.

Lemma B.3. Let $m \in \mathbb{N}^*$, $S \in \mathcal{Z}^m$, and $\mathcal{W} \subset \mathbb{R}^d$ be a finite set. Assume that Assumption 4.2 and that $\ell(\cdot, z)$ is L -Lipschitz continuous on \mathcal{W} for all $z \in \mathcal{W}$. For any $\alpha \in (0, 1]$, we have:

$$\mathbf{Rad}_S(\mathcal{W}) \leq \frac{B}{\sqrt{m}} + B\sqrt{\frac{2 \log(1 + K_{n,\alpha} \mathbf{E}^\alpha(\mathcal{W}))}{m}},$$

with $K_{n,\alpha} := 2(2L\sqrt{n}/B)^\alpha$.

Proof. This result is a particular case of a bound by Andreeva et al. (2024) as part of the proof of their Theorem 3.4. The assumptions of (Andreeva et al., 2024, Theorem 3.4) are satisfied by Assumption 4.2, the Lipschitz continuity assumption, and by considering the Euclidean distance of \mathbb{R}^d as a pseudometric on \mathcal{W} . \square

The second lemma relates the Rademacher complexity to the positive magnitude introduced by Andreeva et al. (2024).

1134 **Lemma B.4.** Let $m \in \mathbb{N}^*$, $S \in \mathcal{Z}^m$, and $\mathcal{W} \subset \mathbb{R}^d$ be a finite set. Assume that Assumption 4.2 holds
 1135 and that $\ell(\cdot, z)$ is L -Lipschitz continuous on \mathcal{W} for all $z \in \mathcal{W}$. Then, we have for any $\lambda > 0$ that:

$$1137 \quad \mathbf{Rad}_S(\mathcal{W}) \leq \frac{\lambda B^2}{2m} + \frac{1}{\lambda} \log (\mathbf{PMag}(L\lambda\mathcal{W})).$$

1139 This result was obtained in the proof of (Andreeva et al., 2024, Theorem 3.5) under a quite general
 1140 Lipschitz regularity condition. For the sake of completeness, we present the proof in our particular
 1141 case, as it might be more concrete for some readers.

1142 *Proof.* Let us fix $S := (z_1, \dots, z_m) \in \mathcal{Z}^m$.

1144 It was shown by Meckes (2015) that a finite set \mathcal{W} has magnitude. More precisely, for any $\lambda > 0$
 1145 there exists a vector $\beta_s : \mathcal{W} \rightarrow \mathbb{R}$, such that for any $a \in \mathcal{W}$ we have:

$$1146 \quad 1 = \sum_{b \in \mathcal{W}} e^{-\lambda \|a-b\|} \beta_\lambda(b).$$

1148 Let $\epsilon = (\epsilon_1, \dots, \epsilon_m) \sim \mathcal{U}(\{-1, 1\})^{\otimes m}$ be Rademacher random variables (see Definition A.1). By
 1149 Lipschitz continuity, we have for all $a \in \mathcal{W}$ that

$$1151 \quad 1 \leq \sum_{b \in \mathcal{W}} e^{-\lambda L \|a-b\|} \beta_{\lambda L}(b)_+$$

$$1153 \quad \leq \sum_{b \in \mathcal{W}} \exp\left(-\frac{\lambda}{m} \sum_{i=1}^m |\ell(a, z_i) - \ell(b, z_i)|\right) \beta_{\lambda L}(b)_+$$

$$1156 \quad \leq \sum_{b \in \mathcal{W}} \exp\left(-\frac{\lambda}{m} \sum_{i=1}^m \epsilon_i (\ell(a, z_i) - \ell(b, z_i))\right) \beta_{\lambda L}(b)_+.$$

1158 Therefore:

$$1160 \quad \exp\left(\frac{\lambda}{m} \sum_{i=1}^m \epsilon_i \ell(a, z_i)\right) \leq \sum_{b \in \mathcal{W}} \exp\left(\frac{\lambda}{m} \sum_{i=1}^m \epsilon_i \ell(b, z_i)\right) \beta_{\lambda L}(b)_+. \quad (10)$$

1162 We apply it to the following choice of a :

$$1164 \quad a = a(\epsilon) := \arg \max_{a \in \mathcal{W}} \frac{\lambda}{m} \sum_{i=1}^m \epsilon_i \ell(a, z_i).$$

1166 Thus, by Jensen's inequality, we have:

$$1168 \quad \mathbf{Rad}_S(\mathcal{W}) = \mathbb{E}_\epsilon \left[\max_{a \in \mathcal{W}} \frac{1}{m} \sum_{i=1}^m \epsilon_i \ell(a, z_i) \right]$$

$$1171 \quad = \mathbb{E}_\epsilon \left[\frac{1}{m} \sum_{i=1}^m \epsilon_i \ell(a(\epsilon), z_i) \right]$$

$$1174 \quad \leq \frac{1}{\lambda} \log \mathbb{E}_\epsilon \left[\exp\left(\frac{\lambda}{m} \sum_{i=1}^m \epsilon_i \ell(a(\epsilon), z_i)\right) \right]$$

$$1177 \quad \leq \frac{1}{\lambda} \log \mathbb{E}_\epsilon \left[\sum_{b \in \mathcal{W}} \exp\left(\frac{\lambda}{m} \sum_{i=1}^m \epsilon_i \ell(b, z_i)\right) \beta_{\lambda L}(b)_+ \right].$$

1179 By Assumption 4.2, independence, and Hoeffding's lemma, we obtain:

$$1180 \quad \mathbf{Rad}_S(\mathcal{W}) \leq \frac{1}{\lambda} \log \sum_{b \in \mathcal{W}} \prod_{i=1}^m \exp\left(\frac{4B^2\lambda^2}{8m^2}\right) \beta_{\lambda L}(b)_+$$

$$1183 \quad = \frac{1}{\lambda} \log \left(\exp\left(\frac{B^2\lambda^2}{2m}\right) \sum_{b \in \mathcal{W}} \beta_{\lambda L}(b)_+ \right)$$

$$1186 \quad = \frac{\lambda B^2}{2m} + \frac{1}{\lambda} \log \mathbf{PMag}(L\lambda \cdot \mathcal{W}),$$

1187 which is the desired result. \square

1188 We can finally prove Theorem 4.4.
 1189
 1190 **Theorem 4.4.** *Suppose that Assumptions 4.2, 3.1, and 4.1 hold. We further assume that the set*
 1191 $\mathcal{W}_{S,U}$ *is almost surely finite. Without loss of generality, assume that $\beta_n^{-2/3}$ is an integer divisor of*
 1192 *n. Then, for any $\alpha \in (0, 1]$, we have*

$$1193 \mathbb{E} \left[\sup_{w \in \mathcal{W}_{S,U}} (\mathcal{R}(w) - \widehat{\mathcal{R}}_S(w)) \right] \leq \beta_n^{1/3} \left(2 + 2B + 2B\mathbb{E} \left[\sqrt{2 \log(1 + K_{n,\alpha} \mathbf{E}^\alpha(\mathcal{W}_{S,U}))} \right] \right),$$

1196 where $K_{n,\alpha} := 2(2L_{S,U}\sqrt{n}/B)^\alpha$. Moreover, for any $\lambda > 0$, let $s(\lambda) := \lambda L_{S,U}\beta_n^{-1/3}/B$. We have

$$1197 \mathbb{E} \left[\sup_{w \in \mathcal{W}_{S,U}} (\mathcal{R}(w) - \widehat{\mathcal{R}}_S(w)) \right] \leq \beta_n^{1/3} \left(2 + \lambda B + \frac{2B}{\lambda} \mathbb{E} [\log \mathbf{PMag}(s(\lambda) \cdot \mathcal{W}_{S,U})] \right).$$

1200 *Proof. Persistent homology bound.* By Lemma 3.4, we have (recall that G_S has been defined in
 1201 Equation (4)):

$$1203 \mathbb{E} [G_S(\mathcal{W}_{S,U})] \leq 2\mathbb{E} [\mathbf{Rad}_{\tilde{S}_J}(\mathcal{W}_{S,U})] + 2J\beta_n,$$

1204 with the notations of Lemma 3.4 for \tilde{S}_J . Now we can apply Lemma B.3 to obtain that:

$$1206 \mathbb{E} [G_S(\mathcal{W}_{S,U})] \leq 2 \left(\frac{B}{\sqrt{J}} + B\mathbb{E} \left[\sqrt{\frac{2 \log(1 + K_{n,\alpha} \mathbf{E}^\alpha(\mathcal{W}_{S,U}))}{J}} \right] \right) + 2J\beta_n,$$

1209 We make the choice $J := \beta_n^{-2/3}$, which we assumed for simplicity is an integer dividing n , so that
 1210 it is a valid choice. This immediately gives the result.

1211 **Positive magnitude bound** By Lemma 3.4, we have (recall that G_S has been defined in Equation (4)):

$$1214 \mathbb{E} [G_S(\mathcal{W}_{S,U})] \leq 2\mathbb{E} [\mathbf{Rad}_{\tilde{S}_J}(\lambda L_{S,U} \mathcal{W}_{S,U})] + 2J\beta_n,$$

1215 with the notations of Lemma 3.4 for \tilde{S}_J . Now we can apply Lemma B.3 to obtain that:

$$1217 \mathbb{E} [G_S(\mathcal{W}_{S,U})] \leq 2\mathbb{E} \left[\inf_{\lambda > 0} \left(\frac{\lambda B^2}{2J} + \frac{1}{\lambda} \log(\mathbf{PMag}(\lambda L_{S,U} \mathcal{W}_{S,U})) \right) + 2J\beta_n \right].$$

1219 We make the change of variable $\lambda \rightarrow \lambda\sqrt{J}/B$, which gives that for any $\lambda > 0$, we have:

$$1221 \mathbb{E} [G_S(\mathcal{W}_{S,U})] \leq \mathbb{E} \left[\frac{\lambda B}{\sqrt{J}} + \frac{2B}{\lambda\sqrt{J}} \log \mathbf{PMag} \left(\frac{\lambda L_{S,U}\sqrt{J}}{B} \mathcal{W}_{S,U} \right) + 2J\beta_n \right].$$

1224 We make the choice $J := \beta_n^{-2/3}$, which we assumed for simplicity is an integer dividing n , so that
 1225 it is a valid choice. This immediately gives the result. \square

1226 To complete this section, we also show Lemma 3.2

1229 B.6 PROOF OF LEMMA 3.2

1231 **Lemma 3.2.** *Consider a fixed $K \in \mathbb{N}^*$, $1 \leq k \leq K$, and algorithms⁵ $\mathcal{A}_k(S, U) := w_k$. Let*
 1232 $\mathcal{A}(S, U) = \mathcal{W}_{S,U} = \{\mathcal{A}_k(S, U)\}_{k=1}^K$ *be an algorithm in the sense of Equation (3). Assume that for*
 1233 *all k , \mathcal{A}_k is δ_k -uniformly argument-stable in the sense of Definition 2.1 and that the loss $\ell(w, z)$ is L -*
 1234 *Lipschitz-continuous in w . Then, \mathcal{A} is random set stable with parameter at most $\beta_n = L \sum_{k=1}^K \delta_k$.*

1235 *Proof.* Consider a data-dependent selection of \mathcal{A} , denoted $\omega(\mathcal{W}, S)$, in the sense of Definition 3.1.
 1236 We consider a measurable mapping $\omega' : \text{CL}(\mathbb{R}^d) \times \mathbb{R}^d \rightarrow \mathbb{R}^d$ such that for any closed set $\mathcal{W} \subset \mathbb{R}^d$
 1237 and any $w \in \mathbb{R}^d$, we have:

$$1239 \omega'(\mathcal{W}, w) \in \arg \min_{w' \in \mathcal{W}} \left(\sup_{z \in \mathcal{Z}} |\ell(w, z) - \ell(w', z)| \right).$$

1241 ⁵ \mathcal{A}_k is an algorithm with values in \mathbb{R}^d , i.e., its output is the k -th iterate of the optimization algorithm.

Such a mapping can be constructed in our setting where the sets are compact and the loss continuous. Consider two datasets S, S' in \mathcal{Z}^n differing by J elements. Let us denote:

$$\varepsilon := \sup_{z \in \mathcal{Z}} \mathbb{E}_U [|\ell(\omega(\mathcal{W}_{S,U}, S), z) - \ell(\omega'(\mathcal{W}_{S',U}, \omega(\mathcal{W}_{S,U}, S)), z)|]$$

We use the definition of ω' and the Lipschitz-continuity of ℓ to obtain that:

$$\begin{aligned} \varepsilon &\leq \sup_{z \in \mathcal{Z}} \mathbb{E}_U \left[\max_{1 \leq k \leq K} |\ell(\mathcal{A}_k(S, U), z) - \ell(\omega'(\mathcal{W}_{S',U}, \mathcal{A}_k(S, U)), z)| \right] \\ &\leq \sup_{z \in \mathcal{Z}} \sum_{k=1}^K \mathbb{E}_U [|\ell(\mathcal{A}_k(S, U), z) - \ell(\omega'(\mathcal{W}_{S',U}, \mathcal{A}_k(S, U)), z)|] \\ &\leq \sum_{k=1}^K \mathbb{E}_U \left[\sup_{z \in \mathcal{Z}} |\ell(\mathcal{A}_k(S, U), z) - \ell(\omega'(\mathcal{W}_{S',U}, \mathcal{A}_k(S, U)), z)| \right] \\ &\leq \sum_{k=1}^K \mathbb{E}_U \left[\sup_{z \in \mathcal{Z}} |\ell(\mathcal{A}_k(S, U), z) - \ell(\mathcal{A}_k(S', U), z)| \right] \\ &\leq L \sum_{k=1}^K \mathbb{E}_U [\|\mathcal{A}_k(S, U) - \mathcal{A}_k(S', U)\|] \\ &= LJ \sum_{k=1}^K \delta_k, \end{aligned}$$

where the last step follows by applying the stability assumption J times and the triangle inequality. The result follows by definition of the random trajectory stability assumption. \square

C ADDITIONAL EXPERIMENTAL DETAILS

This section expands on our experimental analysis, providing additional discussion of the methodology, implementation details, and technical setup.

C.1 IMPLEMENTATION DETAILS

We implement training and validation loops in PyTorch Lightning Version 2.4 using pytorch version 2.4.1. Both models are trained using the AdamW optimizer with a cosine annealing learning rate scheduler. The training was stopped after reaching an accuracy of 95%. No regularization techniques were used to prevent confounding factors in each fine-tuning task.

Vision Transformer (ViT). The ViT is configured for image classification on the CIFAR100 dataset. For the Vision Transformer on CIFAR100, we utilize a model with approximately 1.2 million parameters. This represents a reduction in size compared to the ViT experiments in Andreeva et al. (2024), as the empirical analyses we conduct require substantially more experiments due to the expansion of training set size n and thus storage of weight iterates.

The ViT processes 32x32 pixel images with 3 color channels, and a patch size of 4x4. The transformer backbone consists of 6 layers, 8 attention heads and an MLP dimension of 512. Dropout rates are set to 0.1 within the transformer blocks. Training is performed with a base learning rate of 0.0005, decaying to a minimum of 10^{-5} via cosine annealing.

GraphSage. We analyze GraphSAGE Hamilton et al. (2017) on the graph classification task for MNISTSuperpixels Monti et al. (2017). This model consists of approximately 0.2 million parameters. It processes graphs where each node has a single input feature. These features are initially projected to a hidden dimension of 128. For graph-level predictions, node embeddings are aggregated using ‘mean’ global pooling, followed by a linear layer for classification into 10 classes. The model uses 2-dimensional positional encodings (representing x,y coordinates), which are added to the node features. We use 4 GraphSAGE convolutional layers with a dropout rate of 0.05, a base learning rate of 0.001, and weight decay of 0.0005 to achieve an adequate generalization gap.

1296 C.2 STABILITY ANALYSIS
1297

1298 We first elaborate on our procedure to estimate random set stability in Section 5. The overall al-
1299 gorithm, a proxy to asses Section 5, is summarized in Algorithm 1. Stability experiments were
1300 performed with a fixed learning rate (η) and batch size (b), while varying random seeds (e.g.
1301 $\{100, 200, 300, 400, 500\}$). The same setup is then conducted twice: once with the replacement
1302 set of size $J = 50$, and once without. Since Assumption 3.1 requires taking the supremum over all
1303 samples $Z \in \mathcal{Z}$, we approximate it by evaluating the stability parameter on 500 samples seen during
1304 training and 500 unseen samples. In Table 1, we report the maximum value across both sets.

1305 **Algorithm 1** Stability Parameter Estimation
1306

```

1307 Require:  $S = \{z_1, \dots, z_n\}$ 
1308 Require:  $S_J = \{z'_1, \dots, z'_J\}$ 
1309 Require:  $S_J \cap S = \emptyset$ 
1310 Require:  $J \leq n$ 
1311 1: procedure PROCEDURE(Training)
1312 2: Let  $I = \{i_1, \dots, i_J\}$  be an uniformly random subset of  $\{1, \dots, n\}$  ▷ Indices to replace
1313 3:  $S_{new} := S \setminus \{z_i : i \in I\} \cup S_J := \{z_{new,1}, \dots, z_{new,n}\}$ 
1314 4: Generate  $\mathcal{W}_{S,U}$  with  $|\mathcal{W}_{S,U}| = T$ 
1315 5: Generate  $\mathcal{W}_{S_{new},U}$  with  $|\mathcal{W}_{S_{new},U}| = T$ 
1316 6: procedure PROCEDURE(Estimation)
1317 7:  $M = \min\{n, 500\}$ 
1318 8:  $L = \{j_1, \dots, j_M\}$  be an uniform random subset of  $\{1, \dots, n\}$ 
1319 9:  $S_{eval} := \{z_{new,i} : i \in L\} \setminus S_J$ 
1320 10:  $N := |S_{eval}| = M - J$ 
1321 11:
1322 12: Initialize  $A^1, \dots, A^N \in \mathbb{R}^{T \times T}$ 
1323 13: Let  $w_l \in \mathcal{W}_{S,U} \forall l \in \{1, \dots, T\}$ 
1324 14: Let  $w_{new,l} \in \mathcal{W}_{S_{new},U} \forall l \in \{1, \dots, T\}$ 
1325 15: Let  $\ell(\cdot, \cdot)$  denote the used loss function.
1326 16:
1327 17: For all  $i \in \{1, \dots, N\}$  compute
1328 18: for  $j \leftarrow 1$  to  $T$  do
1329 19:   for  $l \leftarrow 1$  to  $T$  do
1330 20:      $A_{j,l}^i := |\ell(w_j, Z_i) - \ell(w_{new,l}, Z_i)|$  ▷  $Z_i \in S_{eval}$ 
1331 21:   Now we compute  $A := \frac{1}{N} \sum_{i=1}^N A^i$ 
1332 22:
1333 23:   Now we take the minimum over each row in matrix  $A$ 
1334 24:   Initialize  $a \in \mathbb{R}^T$  and compute
1335 25:   for  $m \leftarrow 1$  to  $T$  do  $a_m = \min_{1 \leq l \leq T} A_{m,l}$ 
1336 26:   The algorithm ends with  $\max_{1 \leq h \leq m} a_h$ 

```

1337 C.3 BOUND ESTIMATION
1338

1339 In the first part of Section 5, we estimate the Rademacher complexity bound stated in Lemma 3.4.
1340 In particular, we optimize the quantity
1341

$$1342 2\sqrt{\frac{2\log T}{J}} + 2J\beta_n,$$

1344 which is minimized at

$$1345 1346 J^* = 2^{-\frac{1}{3}} \beta_n^{-\frac{2}{3}} (\log T)^{-\frac{1}{3}}.$$

1347 Since J must be a divisor of the sample size n (see Lemma 3.4), we define the effective choice of J
1348 as

$$1349 J = \arg \min_{d|n} |d - J^*|.$$

1350 C.4 TOPOLOGICAL COMPLEXITY ANALYSIS
13511352 In this section we detail our approach for weight trajectory analysis in terms of topological quantities,
1353 particularly experiments which demonstrate the relationship between stability and our topological
1354 complexity.1355 Following Andreeva et al. (2024), we fine-tune each model from a local minimum for an additional
1356 5000 iterations after training to convergence. We use a reduced parameter grid of 4×4 for η and
1357 b (Andreeva et al. (2024) use 6×6), due to computational constraints arising from the varying the
1358 training set size n . Detailed hyperparameters are listed in Table 2.

1360 Hyperparameter	1361 Vision Transformer	1362 GraphSage
1361 Sample Size (n)	1362 $\{100, 500, 1000, 5000, 10000\}$	1363 $\{100, 500, 1000, 5000, 10000\}$
1362 Learning Rate (η)	1363 $\{10^{-6}, 10^{-5}, 5 \times 10^{-5}, 10^{-4}\}$	$\{10^{-5}, 10^{-4}, 5 \times 10^{-4}, 10^{-3}\}$
1363 Batch Size (b)	1364 $\{32, 64, 128, 256\}$	$\{32, 64, 128, 256\}$

1364 Table 2: Summary of hyperparameter configurations for Vision Transformer and GraphSage models.
13651366 C.5 HARDWARE AND RUNTIME
13671368 Models are trained on a cluster with 40GB A40/A100 GPUs; although the experiments are repro-
1369ducible with lower memory requirements. For our grid experiments, computing topological features
1370 alongside hyperparameter variations (sample size, learning rate, and batch size) demanded approx-
1371imately 57 GPU hours for GraphSage and 140 GPU hours for the Vision Transformer (ViT). In
1372 contrast, the stability analysis required about 50 total GPU hours.
13731374 D ADDITIONAL EMPIRICAL RESULTS
13751376 In this section, we present additional empirical results. The first part complements the second part
1377 of Section 5. In the main text, we focused on the α -weighted lifetime sum in Theorem 4.4. The
1378 second bound, given in terms of the positive magnitude \mathbf{PMag} will be discussed here.
13791380 Motivated by the dependence of the stability parameter in Assumption 3.1 on the sample size n , we
1381 also investigate the topological complexity measures introduced in Theorem 4.4. To the best of our
1382 knowledge, this behavior has not been addressed in previous work. We study it here to provide a
1383 more complete picture of the α -weighted lifetime sum and the positive magnitude.
13841385 D.1 INTERPLAY BETWEEN STABILITY AND $\mathbf{C}(\mathcal{W}_{S,U})$
13861387 In this subsection, in addition to the results presented in Section 5, we provide the results specifically
1388 for the *positive magnitude*. The second bound in Theorem 4.4 depends on the scaling parameter
1389 $s(\lambda)$. Recall that in Theorem 4.4, the parameter $s(\lambda)$ can be chosen arbitrarily. The theoretically
1390 justified choice is $s(\lambda) = \mathcal{O}(n^{-1/3})$ in order to obtain the optimal convergence rate. Nevertheless,
1391 alternative choices of $s(\lambda)$ have also led to remarkable correlation results in previous work Andreeva
1392 et al. (2024). We focus on the setting $s(\lambda) = n^{-1/3}$ with $n \in \{100, 10^4\}$.
13931394 **Results and Discussion.** We observe the same behavior as in the main text (Section 5). We note
1395 that the effects for GraphSage Figure 4 and Figure 5 are less pronounced than for the ViT (Figure 6
1396 and Figure 7); nonetheless, the general trend remains visible. Interestingly, for $s(\lambda) = 0.01$, we
1397 observe a different behavior. While for higher values of $s(\lambda)$ the steepness varies with the sample
1398 size, as predicted by Theorem 4.4 and also observed for \mathbf{E}^1 , the steepness remains consistent across
1399 different values of n .1400 The same behavior for $\mathbf{PMag}(s(\lambda) \cdot \mathcal{W}_{S,U})$, with $s(\lambda) = n^{-\frac{1}{3}}$, can be explained theoretically. In
1401 Theorem 4.4, we observe the product structure. Indeed, Theorem 4.4 asserts that $\log \mathbf{E}^1(\mathcal{W}_{S,U})$
1402 should be approximately of order at least $\beta_n^{-1/3} G_S(\mathcal{W}_{S,U})$, which corresponds to $n^{1/3} G_S(\mathcal{W}_{S,U})$
1403 when $\beta_n = \Theta(1/n)$. Therefore, our experimental results provide strong empirical support for
Theorem 4.4 both for \mathbf{E}^1 and \mathbf{PMag} .

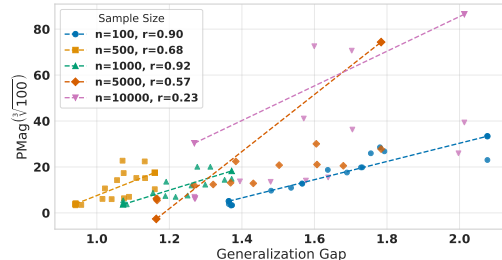


Figure 4: Variation of $\text{PMag}(\sqrt[3]{100} \cdot \mathcal{W}_{S,U})$ with sample size n for the model **GraphSage**. Pearson correlation coefficients r are reported for each subgroup.

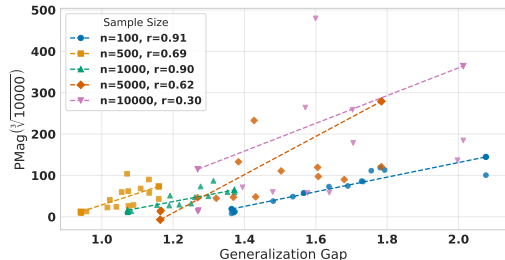


Figure 5: Variation of $\text{PMag}(\sqrt[3]{10000} \cdot \mathcal{W}_{S,U})$ with sample size n for the model **GraphSage**. Pearson correlation coefficients r are reported for each subgroup.

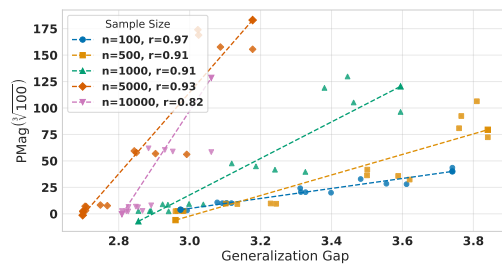


Figure 6: Variation of $\text{PMag}(\sqrt[3]{100})$ with sample size n for the model **ViT**. Pearson correlation coefficients r are reported for each subgroup.

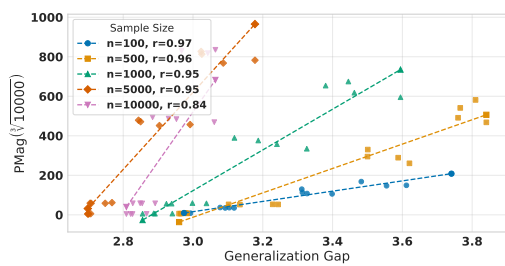


Figure 7: Variation of $\text{PMag}(\sqrt[3]{10000})$ with sample size n for the model **ViT**. Pearson correlation coefficients r are reported for each subgroup.

D.2 COMPLEXITY MEASURES $\mathbf{C}(\mathcal{W}_{S,U})$ AS FUNCTIONS OF THE SAMPLE SIZE n

While the main write-up in Section 5 focused on order of the bound values of Lemma 3.4 and overall behavior, in this section we investigate the behavior of the topological complexity measure introduced in Andreeva et al. (2024). In particular, in Theorem 4.4 we recover the same complexity measures $\mathbf{C}(\mathcal{W}_{S,U})$ within our stability framework. Motivated by the dependence of the stability parameter in Assumption 3.1 on the sample size n , we investigate the *positive magnitude* and the α -weigthed lifetime sum with respect to the training data size.

Experimental Design. Similarly to Section 5, we investigate the behavior of two conceptually different models: a Vision Transformer (**ViT**) and **GraphSage**. The implementation details remain consistent with the main experimental setting. In particular, we analyze the behavior of $\mathbf{E}^1(\mathcal{W}_{S,U})$ as a function of the sample size n , for fixed learning rates $\eta = 10^{-4}$ and $\eta = 10^{-5}$ for ViT, and $\eta = 10^{-3}$ and $\eta = 10^{-4}$ for GraphSage, across all batches. Our focus is on $\mathbf{E}^1(\mathcal{W}_{S,U})$ and $\text{PMag}(s(\lambda) \cdot \mathcal{W}_{S,U})$, with $s(\lambda) = n^{\frac{1}{3}}$ and $n \in \{100, 10^4\}$.

Results and Discussion. For fixed learning rates, we observe that both \mathbf{E}^1 and PMag increase with increasing n and appear to stabilize for large values of n (see Figures 9, 8, 11, 10, 13, 12). This suggests a relationship between the sample size and the topology of the training trajectory, a phenomenon that has not been previously highlighted in the literature.

At first glance, the increase of $\mathbf{E}^1(\mathcal{W}_{S,U})$ with n may seem counterintuitive, since we typically expect generalization error (and related bounds) to decrease as the sample size grows. However, this behavior is consistent with theory: the α -weigthed lifetime sum is expected to grow at most polynomially with n . The positive magnitude remains bounded in terms of the number of iterations.

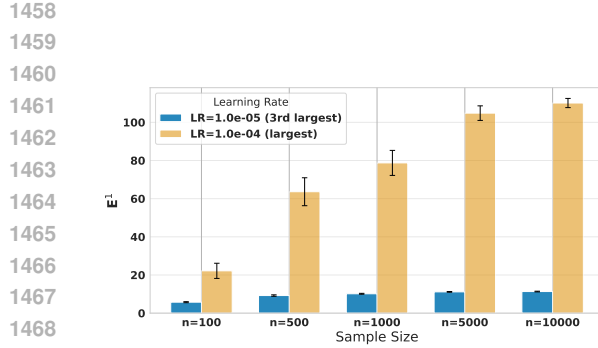


Figure 8: Evolution of $E^1(\mathcal{W}_{S,U})$ with increasing sample size n , for learning rates $\eta = 10^{-5}$ and $\eta = 10^{-4}$ (**ViT**).

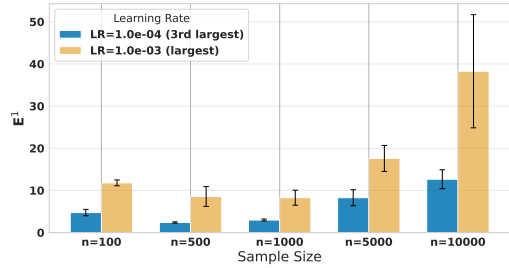


Figure 9: Evolution of $E^1(\mathcal{W}_{S,U})$ with increasing sample size n , for learning rates $\eta = 10^{-3}$ and $\eta = 10^{-4}$ (**GraphSage**).

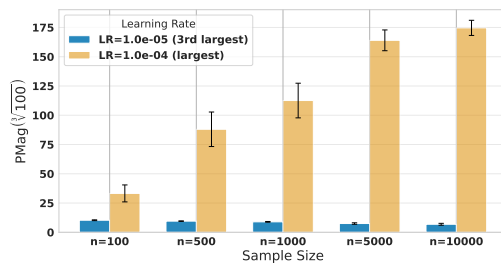


Figure 10: Evolution of $\text{PMag}(\sqrt[3]{100} \cdot \mathcal{W}_{S,U})$ with increasing sample size n , for learning rates $\eta = 10^{-5}$ and $\eta = 10^{-4}$ (**ViT**).

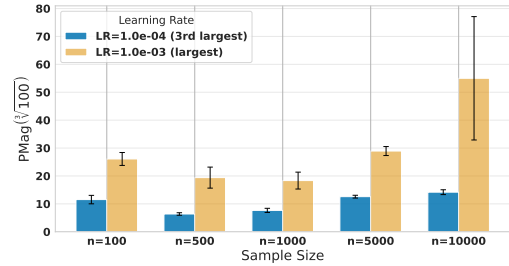


Figure 11: Evolution of $\text{PMag}(\sqrt[3]{100} \cdot \mathcal{W}_{S,U})$ with increasing sample size n , for learning rates $\eta = 10^{-3}$ and $\eta = 10^{-4}$ (**GraphSage**).

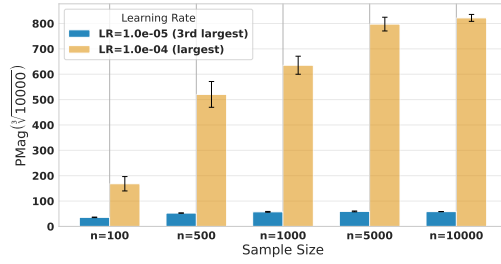


Figure 12: Evolution of $\text{PMag}(\sqrt[3]{10000} \cdot \mathcal{W}_{S,U})$ with increasing sample size n , for learning rates $\eta = 10^{-4}$ and $\eta = 10^{-4}$ (**ViT**).

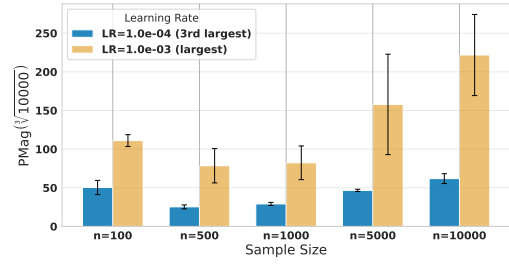


Figure 13: Evolution of $\text{PMag}(\sqrt[3]{10000} \cdot \mathcal{W}_{S,U})$ with increasing sample size n , for learning rates $\eta = 10^{-3}$ and $\eta = 10^{-4}$ (**GraphSage**).